


For Reference

NOT TO BE TAKEN FROM THIS ROOM

Ex libris
UNIVERSITATIS
ALBERTAENSIS





Digitized by the Internet Archive
in 2020 with funding from
University of Alberta Libraries

<https://archive.org/details/Cox1979>

THE UNIVERSITY OF ALBERTA

RELEASE FORM

NAME OF AUTHOR ... John Cox

TITLE OF THESIS ... The Geology of the Northwest Margin of the
... Nelson Batholith, British Columbia.

DEGREE FOR WHICH THESIS WAS PRESENTED ... Master of Science

YEAR THIS DEGREE GRANTED ... 1979

Permission is hereby granted to THE UNIVERSITY OF
ALBERTA LIBRARY to reproduce single copies of this thesis
and to lend or sell such copies for private, scholarly or
scientific research purposes only.

The author reserves other publication rights, and
neither the thesis nor extensive extracts from it may be
printed or otherwise reproduced without the author's
written permission.

THE UNIVERSITY OF ALBERTA

THE GEOLOGY OF THE NORTHWEST MARGIN OF
THE NELSON BATHOLITH, BRITISH COLUMBIA.

BY



JOHN COX

A THESIS

SUBMITTED TO THE FACULTY OF GRADUATE STUDIES AND RESEARCH
IN PARTIAL FULFILMENT OF THE REQUIREMENTS FOR THE DEGREE
OF MASTER OF SCIENCE

DEPARTMENT ...GEOLOGY.....

EDMONTON, ALBERTA

SPRING, 1979

THE UNIVERSITY OF ALBERTA

FACULTY OF GRADUATE STUDIES AND RESEARCH

The undersigned certify that they have read, and recommend
to the Faculty of Graduate Studies and Research, for acceptance,
a thesis entitledTHE GEOLOGY OF THE NORTHWEST MARGIN....
.....OF THE NELSON BATHOLITH, BRITISH COLUMBIA.....
.....
submitted byJOHN COX.....
in partial fulfilment of the requirements for the degree of
Master of ...SCIENCE.....

ABSTRACT

The Nelson batholith and its associated satellites intrude the argillaceous Slocan Group sediments in the southern Omineca Crystalline Belt of southeast British Columbia. Both the batholith and the country rock are cut by Pb-Zn-Ag bearing veins which have been economically important since the turn of the century. Twenty-four samples from the batholith and 100 samples from the sediments were analysed for major and trace elements and the isotopic abundances of nine ore-lead samples were determined.

Near to its northwest margin the Nelson batholith is composed mainly of granodiorite with a more mafic border phase, while xenoliths of basic material are contained within the granodiorite. Plagioclase porphyry satellite bodies intrude the sediments to the north of the contact and the majority of the igneous rocks exhibit the effects of late stage hydrothermal alteration. The intrusive differentiated from a calc-alkaline magma and the common presence of hornblende, the wide range in SiO_2 content and the relatively low initial $^{87}\text{Sr}/^{86}\text{Sr}$ ratios of the rocks classify the batholith as an I-type granitoid which probably originated in the mantle wedge above a subduction zone in the Middle Jurassic.

The Slocan Group sediments are predominantly distal turbidites of varied chemical composition with rarer calcareous, quartzitic and tuffaceous horizons. In the highest part of the sequence they were derived from a basic source, whilst lower down the Group they had a more highly siliceous source region. There is no geochemical evidence that the ore metals were derived from the Slocan Group sediments.

The ore-lead is shown to be of dual origin with that from the Ainsworth and Bluebell camps being derived, at least in part, from the Precambrian basement whilst the lead from deposits further west and from

K-feldspar in the batholith is of 'young' oceanic affinity. This is taken as evidence that the western edge of the Precambrian basement underlies the vicinity of Kootenay Lake.

The geology of the area is fitted into the general island arc tectonic model for the region during Upper Triassic to Middle Jurassic times. An easterly dipping subduction zone generated both the Rossland volcanics island arc, a possible source for the basic Slocan sediments, and the Nelson batholith whose associated hydrothermal system was the source of the ore deposits in the region.

ACKNOWLEDGEMENTS

My thanks go to the many people for help in the preparation of this thesis. Without the substantial aid and guidance of Dr. Lambert the work would have been neither started nor completed. Dr. Holland and Ron Hardy in Durham performed the X.R.F. analyses and Dr. Baadsgaard carried out the isotope abundance measurements. Frank Dimitrov, Jenni Blaxley and Alex Stelmach donated their technical skills and the field work would not have been the same without Willy Wagner. Simon Brame has been a constant companion, friend and inspiration.

Finally the Geology department of the University of Alberta provided the teaching assistantship and the opportunity to live in Canada for which I am extremely grateful.

TABLE OF CONTENTS

CHAPTER	PAGE
1 INTRODUCTION	1
1.1 Research Aims	1
1.2 Location of Field Area	1
1.3 History of Research	3
1.4 Regional Setting	4
1.5 General Geology	5
1.6 Sampling and Analytical Techniques	10
2 THE NELSON BATHOLITH	14
2.1 Introduction	14
2.2 Petrology	15
2.3 Geochemistry	20
2.4 Origin of the Nelson Batholith	27
3 THE SLOCAN GROUP	32
3.1 Introduction	32
3.2 Sampling	34
3.3 Chemistry and Provenance	35
3.4 Ore Metals	47
4 LEAD ISOTOPES	53
5 CONCLUSIONS AND DISCUSSION	61

REFERENCES	65

CHAPTER	PAGE
APPENDIX 1. THE NELSON BATHOLITH	
Chemical analyses	71
Approximate modal analyses	75
Norms	77
APPENDIX 2. THE SLOCAN GROUP	
Chemical analyses	79
Mineral assemblages	93
Norms	95

LIST OF TABLES

Table	Description	Page
1	Average chemical analyses for the Slocan Group sediments	37
2	Isotopic composition of lead from galena and pyrite samples from near or within the Nelson batholith	54

LIST OF FIGURES

Figure	Page
1. Location map	2
2. Geological sketch map of southeast British Columbia	6
3. Stratigraphic column for Nelson-Rossland region	7
4. Sample location map	11
5. AFM diagram	21
6. MgO versus SiO ₂ diagram	22
7. V versus Ni diagram	23
8. K ₂ O versus Rb diagram	25
9. FeO (total) versus TiO ₂ diagram	26
10. FeO (total) versus V diagram	28
11. MgO versus V diagram	29
12. Principal Component Matrix factor scores for the Slocan sediments	38
13. K ₂ O: Na ₂ O: CaO diagram	40
14. SiO ₂ versus K/Rb diagram	42
15. TiO ₂ versus Zr diagram	43
16. MgO versus Ni diagram	44
17. MgO versus Cr diagram	45
18. Zn versus Cu diagram	48
19. Fe ₂ O ₃ (total) versus Cu diagram	49
20. Fe ₂ O ₃ (total) versus Zn diagram	50
21. K ₂ O versus Pb diagram	52
22. ²⁰⁷ Pb/ ²⁰⁴ Pb versus ²⁰⁶ Pb/ ²⁰⁴ Pb diagram for the Nelson batholith and associated ore deposits	55
23. Sketch cross sections for the region during Upper Triassic, Lower Jurassic and Middle Jurassic times	64

LIST OF PLATES

Plate	Description	Page
I [1]	Main body granodiorite, hand specimen	16
[2]	Main body granodiorite, thin section	
[3]	Porphyry, hand specimen	
[4]	Porphyry, thin section	
II [1]	Border rock, hand specimen	17
[2]	Border rock, thin section	
[3]	Xenolith, hand specimen	
[4]	Xenolith, thin section	

CHAPTER 1

INTRODUCTION

1.1 Research Aims

The northwest margin of the Nelson batholith, southern British Columbia, has been of geological interest since the turn of the century because of the lead-zinc-silver veins found in both the batholith and the adjacent sediments. The ore deposits have been the subject of intensive study but the host rocks have received comparatively little attention. More recently, the tectonic setting of this region of the Omineca Crystalline Belt during the Mesozoic has come under scrutiny, especially with regard to the position of the western edge of the continental crust during this period of geological time. A geochemical study was therefore undertaken with the object of gaining insight into the source of the sediments, the origin of the batholith and, possibly, the source of the ore metals in the region.

1.2 Location of Field Area

The area of study is situated in southeastern British Columbia near to the intersection of the 50th parallel and the 117th meridian, approximately 50 km north of Nelson (Figure 1). Slocan Lake provides a natural western boundary and the Kaslo-New Denver road a convenient northern limit. No fixed boundaries were chosen to the south and east but the batholith was sampled no further than four miles south of its northern margin and the sediments no further east than Zincton. The greater part of the area falls within the Nelson map-area (west half) whose general geology has

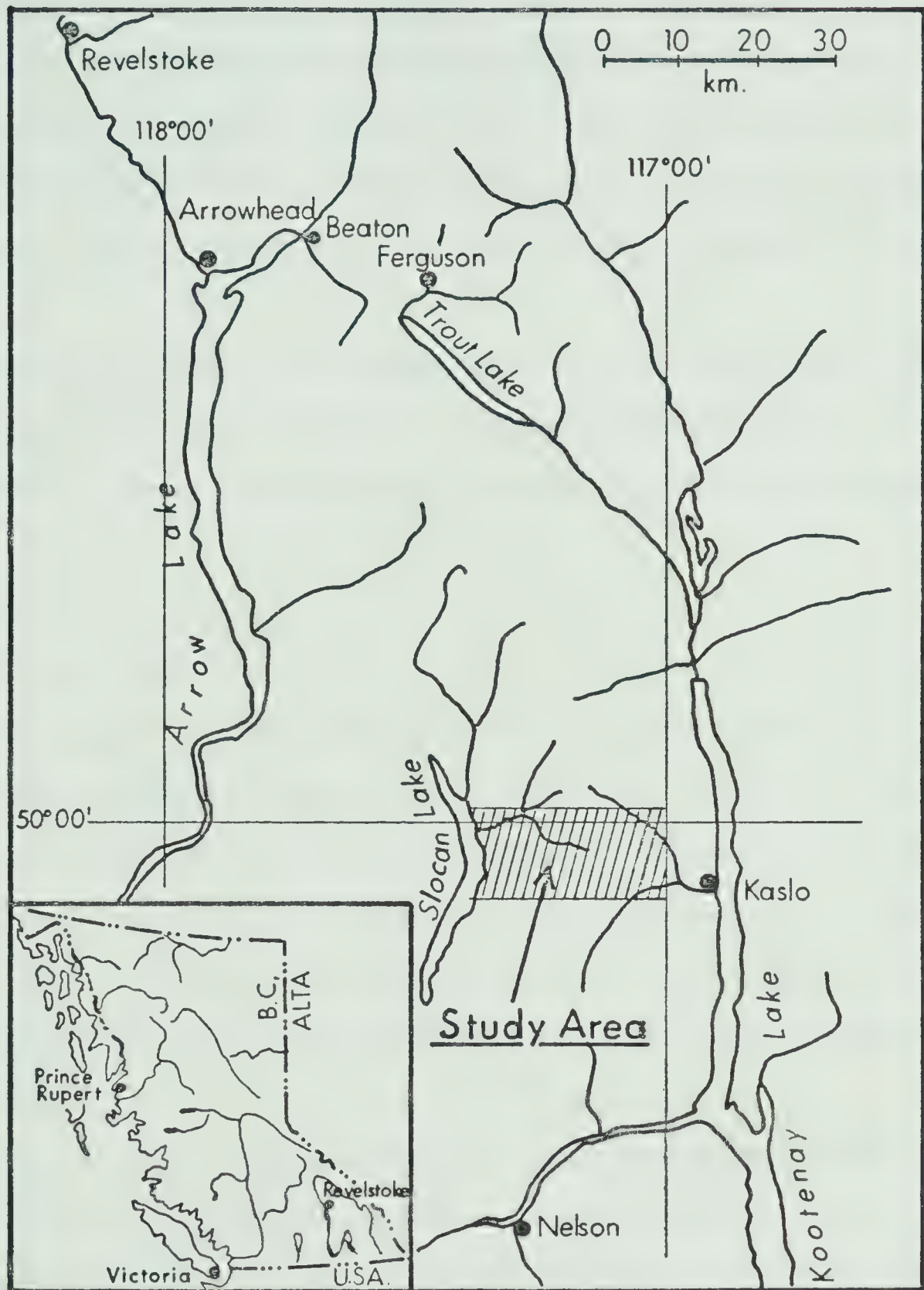


Figure 1. Location Map.

been described by Little (1960).

Physiographically, the area falls in the Slocan range of the Selkirk Mountains. Idaho Peak (2280 m) is the highest point of Silver Ridge, which dominates the region, and is cut by the main valleys of the Carpenter and Silverton Creeks. The mountain slopes are densely vegetated up to around 2000 m and outcrop is limited to road cuttings and river banks.

Access to the area is provided by the Nelson-New Denver and Kaslo-New Denver roads and within the area by numerous old mine tracks, remnants of the days when the ghost town of Sandon housed several thousand people.

1.3 History of Research

The first geological mapping of the region between Kootenay and Slocan Lakes was begun in 1894 by R.G. McConnel and completed in 1900 by R.W. Brock. Mining flourished around the turn of the century and O.E. Leroy and C.W. Drysdale made a study of the Slocan mining camp between 1908 and 1917. Further work by M.F. Bancroft and C.E. Cairnes resulted in the publication of two memoirs and their associated maps (Cairnes 1934, 1935).

Since this time, studies have been carried out on the structure and mineral deposits of the region by members of the Geological Survey of Canada and the British Columbia Department of Mines and Petroleum Resources. More important publications in this group include the works by M.S. Hedley (1952) on the Sandon area, H.W. Little (1960) on the general geology of the Nelson map-area (west half) and J.T. Fyles (1967) on the Ainsworth-Kaslo region.

K.K. Nguyen, A.J. Sinclair and W.G. Libby (1968) have obtained K-Ar dates for the northern part of the Nelson batholith and A.J. Sinclair (1966) performed a lead isotope study on galenas from the area. Further references on most recent works are given in the relevant chapters of the thesis.

1.4 Regional Setting

The area studied lies within the southern part of the Omineca Crystalline Belt, one of the five distinct geological belts paralleling the present continental margin, which make up the Canadian Cordillera.

Rifting in the mid-Proterozoic established the western margin of the North American craton which was situated well east of the present day continental margin. The Proterozoic Purcell and Windermere Super groups were probably deposited as shelf: slope: rise assemblages and Atlantic-type margin deposition continued until terminated by the late Devonian-early Mississippian Caribboan orogeny (Dickinson 1976). The western margin of North America then ceased to be an intraplate boundary, becoming a plate margin as it interacted with a plate to the west (Monger et al 1972). Late Palaeozoic volcanic arcs developed in the Omineca Crystalline Belt. Oceanic rocks occur in the Intermontane Belt to the east and a subduction zone dipped eastwards under the continental margin.

During the Upper Triassic-Lower Jurassic period the subduction zone apparently moved westwards due to the accumulation of material during the previous subduction episode. Extensive volcanics of a predominantly basic nature (Monger 1975) were deposited in an island arc environment along most of the Cordillera. The Nicola, Hazelton and Takla volcanics

fall into this class. Sediment deposition took place in increasingly restricted basins and the flysch like sediments of the Slocan and Ymir Groups accumulated at this time, apparently from a westerly source.

Between the Lower Jurassic and the Upper Cretaceous the emergence of the Cordillera caused a change in regime from the island arc setting, through an intermediary 'successor' basin stage (Douglas et al 1970) to a totally continental Cordillera. The widespread plutonics of the Coast Belt show that subduction continued throughout this time whilst in the Omineca Crystalline Belt the Columbian orogeny produced the intrusion, around 160 Ma ago, of numerous plutons of which the Nelson batholith is one example.

Crustal extension rather than compression has taken place over most of the Cordillera since Miocene time. This sequence of events is comparable to those of the present day Andes of South America.

1.5 General Geology

Rocks ranging in age from Precambrian to Tertiary outcrop in the southern part of the Omineca Crystalline Belt. The outcrop of the Triassic and Jurassic rocks is shown in Figure 2 and the stratigraphic column for the Nelson-Rossland region is shown in Figure 3.

The oldest rocks in the region outcrop to the east of Kootenay Lake. These are the fine clastics and carbonates, up to 14000 m in thickness, of the Purcell Supergroup. They are unconformably overlain by the late Proterozoic Windermere Supergroup which is represented by a series of predominantly coarse clastic beds with intercalated volcanic and calcareous horizons. The Precambrian-Cambrian boundary has been taken by Little (1960) as the base of the lowest formation containing Lower Cambrian fossils: thus the conformable boundary between the Three

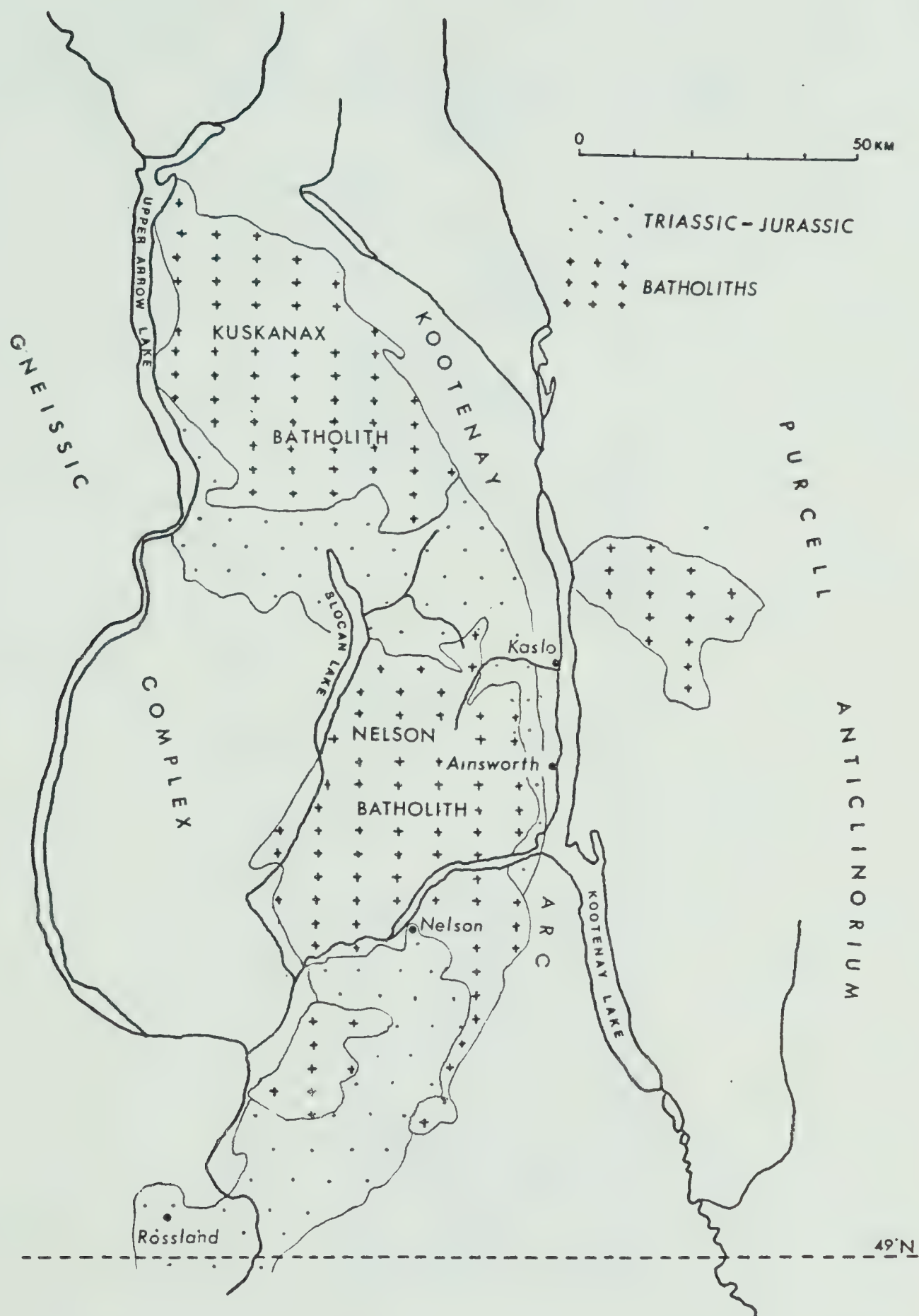


Figure 2. Geological sketch map of southeast British Columbia showing Triassic-Jurassic outcrop in relation to the Nelson batholith.

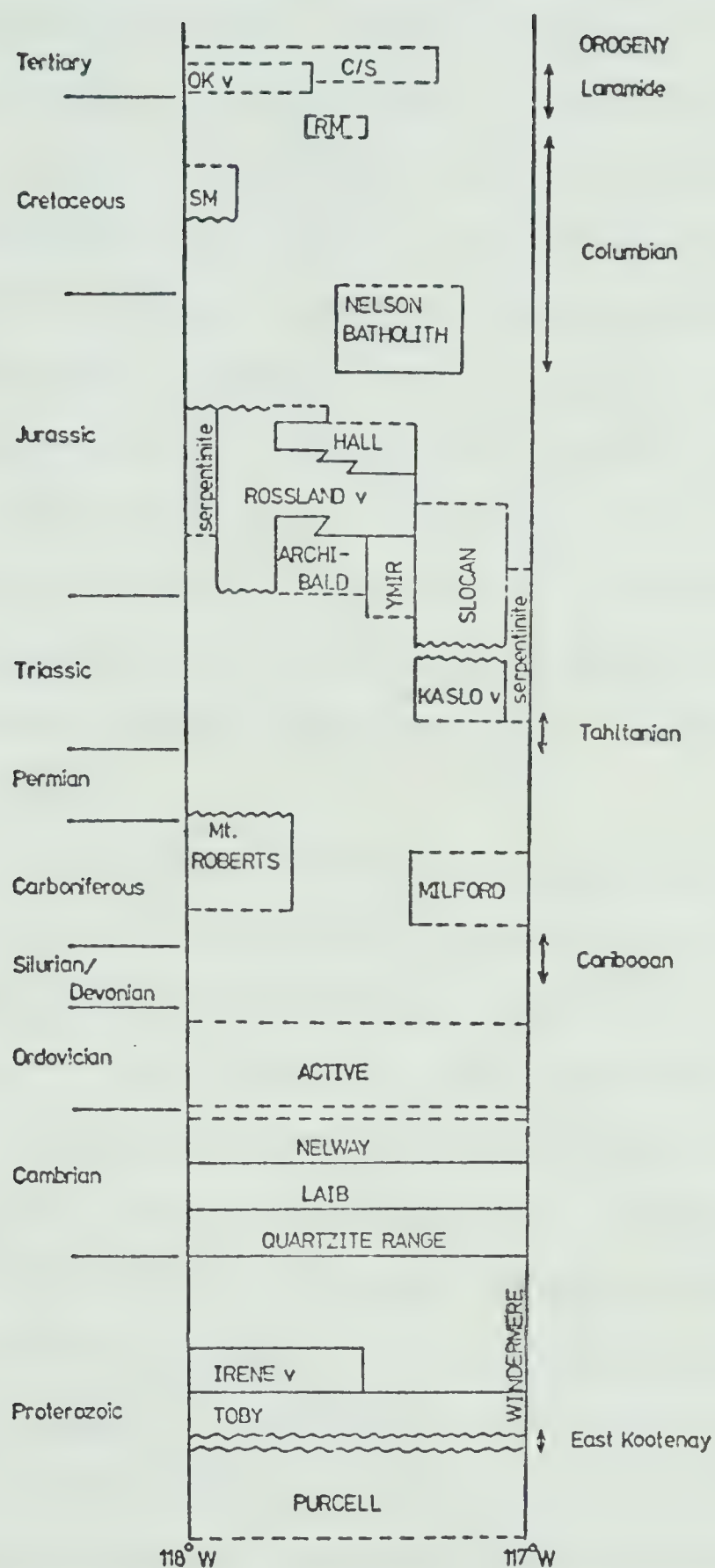


Figure 3. Stratigraphic column for the Nelson-Rossland region after Douglas et al (1970).

Sisters Formation (Windermere) and the Quartzite Range Formation is regarded as the base of the Palaeozoic. Cambrian sedimentation occurred in a shallow sea basin distant from the shoreline as limestones and argillaceous sandstones of the Laib and Nelway Formations were deposited. The Ordovician Active Formation is of similar origin, clastics being derived from a distant easterly landmass. Deposits of Silurian or Devonian age are not found in the region, probably due to the effects of the Caribooan orogeny. Following this period of non deposition came the shallow sea Upper Carboniferous deposits of the Mount Roberts and Milford Formations. The lower members are predominantly limestones with interbedded lavas and tuffs whilst the upper members are mainly argillaceous beds becoming coarser towards the top, probably indicating a marine regression around the onset of the Permian.

Unconformably overlying the Milford Group are the altered volcanics of the Kaslo Group, included by Monger (1975) in a Palaeozoic to Mid-Triassic volcanic arc belt. Fossil evidence in sediments above and below give the Kaslo Group a likely Triassic age. The eugeosynclinal sediments of the Slocan Group unconformably overlies the Kaslo Group (Cairnes 1934): they will be considered in more detail in Chapter 3. Further south are the argillaceous sediments of the Ymir Group. They bear a strong lithological similarity to the Slocan Group and were probably deposited in the same geosynclinal trough. The dominantly volcanic Rossland Group conformably overlies the Ymir sediments. They are Lower to Middle Jurassic in age and are of similar age to the volcanics of the Intermontane Belt to the west where the Lower Jurassic Hazelton Group and Upper Triassic Takla and Nicola Groups are found. According to Beddoe-Stephens (1977) the Rossland volcanics are of island-arc affinity with the magmas ori-

ginating in the upper mantle.

The Hall Formation is both underlain and overlain by the Rossland Group. These upward coarsening sediments, together with the presence of shallow water structures, may reflect the onset of the Columbian orogeny. Apart from very minor conglomeratic horizons, all younger rocks in the region belong to the intrusive igneous group. The Nelson batholith was emplaced during the first half of the Columbian orogeny (Nguyen et al 1968, Gabrielse and Reesor 1974). To the southwest of the Nelson batholith are the Trail, Rossland and Coryell batholiths. Fyles et al (1973) give K-Ar dates on the Trail and Coryell intrusives of 48-50 Ma. Compared to the Nelson batholith they are a more alkaline suite of rocks (Gabrielse and Reesor 1974).

Approximately 20 km west of the area studied lies the western boundary of the Kootenay Arc, a major structural trend of the southern Omineca Crystalline Belt, whose position is shown in Figure 2. The Kootenay Arc is a north-trending metamorphic fold belt which has been mapped from Revelstoke in the north to the Spokane River of northeastern Washington in the south. It is bounded to the east by the Purcell anticlinorium and to the west by the Shuswap Metamorphic Complex and the Nelson and Kuskanax batholiths. Within the arc are complexly folded and faulted strata of Upper Proterozoic, Palaeozoic and Mesozoic age. The central Kootenay Arc is characterised by tight to isoclinal, north-south trending folds superposed on the Riondel Nappe, a westward closing recumbent anticline in the Lower Palaeozoic rocks (Hoy 1976). Winzer (1973) and Hoy (1976) have mapped metamorphic isograds in a zone of medium to high grade regional metamorphism in the Riondel area. Wheeler (1966) believes that the arc may have originated by the squeezing and resultant upwelling of

material between the Nelson and Kuskanax batholiths and the Purcell anticlinorium during the Columbian orogeny.

1.6 Sampling and Analytical Techniques

Samples were taken from the Nelson batholith and its satellite bodies and all were sectioned. Twenty-four of these samples, chosen to include the different rock types found, were then designated for whole rock chemical analysis. Their location is shown in Figure 4. Sediment samples were collected and a representative number were sectioned. In addition batches of twenty samples were taken at approximately 3-5 m intervals from continuous sections in the sediments. Five such batches were collected, with locations as shown on Figure 4, for whole rock chemical analysis.

The samples to be analysed were initially trimmed with a diamond saw to remove the weathered surface. They were then crushed in a jaw crusher before being powdered in a tungsten carbide swing mill.

Lead and vanadium were analysed by atomic absorption spectrophotometry (A.A.S.) at the University of Alberta and the remaining elements were analysed by X-ray fluorescence at the University of Durham. To prepare the samples for A.A.S. analysis 1 gram of the powdered rock was dissolved in 10 mls of HF and 10 mls of HNO_3 and the solution was evaporated down to dryness. Two further 10 ml volumes of HNO_3 were added and each one evaporated to dryness. The soluble residue was then dissolved in a 5% HNO_3 solution, diluted to volume and, where necessary, insoluble graphite was filtered off.

A.A.S. is the study of the absorption of radiant energy by atoms. The technique is useful as it is a highly sensitive method of rapid analysis

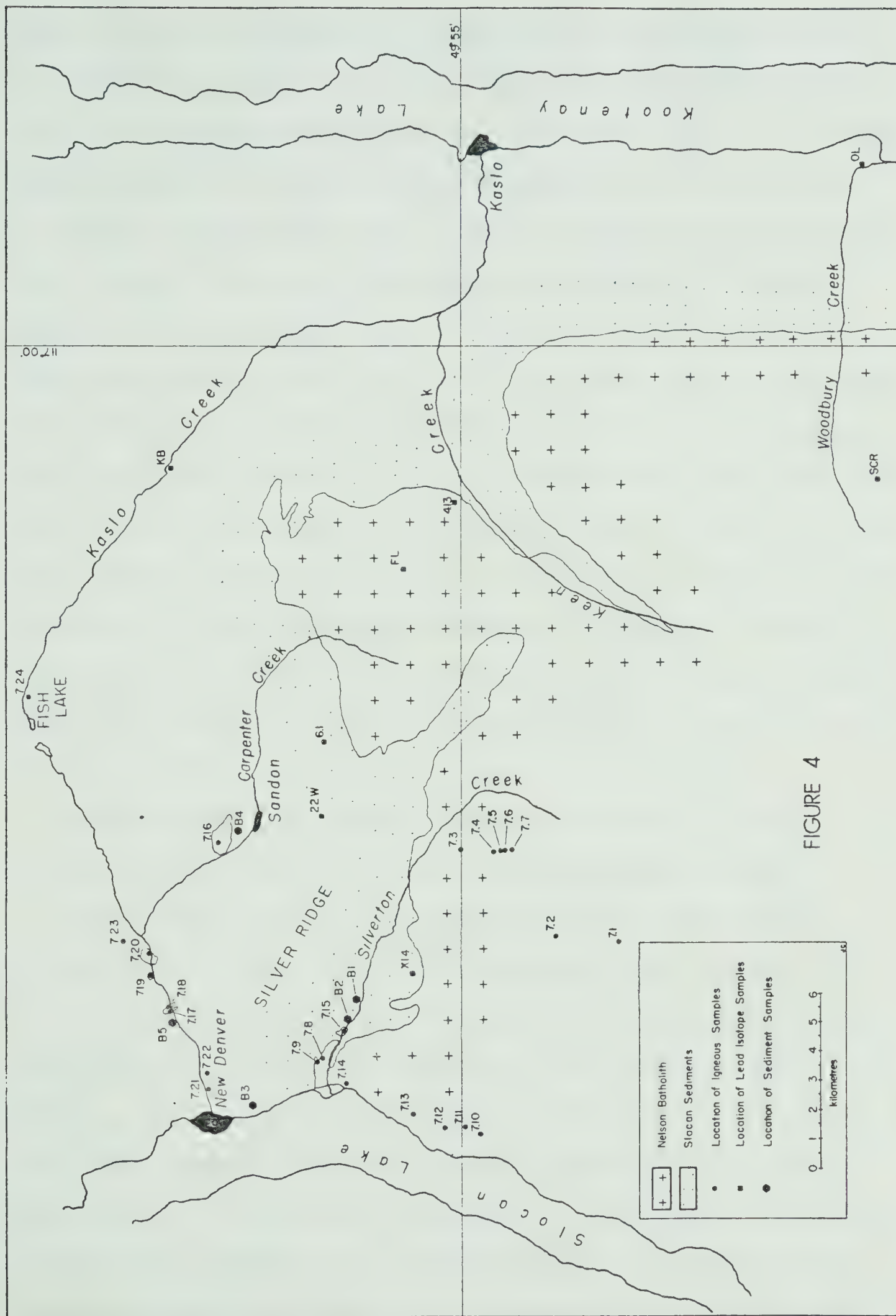


FIGURE 4

which is capable of measuring the trace quantities of elements in rocks. The unexcited or ground state atoms of an element will absorb certain wavelength radiation from excited atoms of the same element. This phenomenon appears to be a predictable and measurable property of the atom. In practice a hollow cathode lamp contains a cathode made out of the desired element. The atoms of the cathode are excited by the heating of argon gas within the cathode lamp. Excited electrons are now in a higher energy state and when they collide with other electrons they loose this energy which is emitted as radiation. The sample, in solution, is then sprayed into an acetylene/air or acetylene/nitrous oxide flame where it is irradiated by a particular isolated wavelength of radiation. The flame reduces a portion of the solution to free atoms of its constituent elements which absorb the emitted radiation. Absorption of radiation is proportional to the amount of sample element present and the non-absorbed radiation is measured by a photomultiplier-amplifier system. The results may be in the form of a digital read-out or a chart recording.

Sample solutions are measured relative to standard solutions of known concentration and of similar acidity to the sample solutions.

Seven galena samples and two pyrite samples were chosen for Pb isotope analysis. The location of the samples is shown in Figure 4. The sulphide was dissolved in vapour distilled HNO_3 and the solution was diluted before the addition of concentrated HNO_3 to directly precipitate $\text{Pb}(\text{NO}_3)_2$. For the low Pb pyrite samples a $\text{Ba}(\text{NO}_3)_2$ carrier was added. Centrifuging separated the precipitate from the solute and the solute was discarded. The residue was dissolved in 1.5N HCl and this solution was purified by passage through an anion exchange column. Pure PbCl_2 crystallised from the solution. This was then picked up in H_3PO_4 and

loaded onto silica gel on a rhenium filament. The isotopic composition of the Pb was then measured on a micromass MM30 mass spectrometer and the isotopic values were corrected for mass discrimination by normalising to the measured ratios of the NBS 981 Pb standard.

CHAPTER 2

THE NELSON BATHOLITH

2.1 Introduction

The Nelson batholith is a heterogeneous granitoid body occupying approximately 2000 km² between Kootenay and Slocan Lakes lying predominantly north of the West arm of Kootenay Lake. Cairnes (1934) described the main mass of the batholith as 'a massive porphyritic granite' but it has since been found that granodiorite is the most common rock type. Towards its contact with the country rock, the massive porphyritic facies becomes less coarsely grained and there is a decrease in the size and number of K-feldspar megacrysts. The specimens collected for this work were taken from such an area, close to the northwest margin of the batholith (Figure 4).

The age of emplacement of the batholith may be bracketed by stratigraphic evidence. The youngest rocks cut by the batholith are the early Middle Jurassic Hall Formation and eroded Nelson pebbles are found in the middle to late Lower Cretaceous Blairmore Formation. This is in agreement with ages from radioactive isotope studies.

K-Ar isotopic age determinations, according to Gabrielse and Reesor (1964), fall into three groups which together with structural evidence supports the following sequence of events.

1. "Emplacement and consolidation of a large massif of hornblende-biotite granodiorite before 171 Ma, at a greater structural depth than now exists.

2. "Mobilisation and reintrusion ... resultant upon an intense structural episode that affected the region generally ... at, or later than 131 Ma ... and may, in fact, be the fundamental cause of the development of the Kootenay Arc.

3. "Further emplacement of leucocratic quartz monzonite in and around the fringe of the batholith" giving ages around 55 Ma.

Recent Rb/Sr whole rock isochron dates (Duncan, Parrish and Armstrong 1979) are in approximate agreement with the K/Ar age determinations. A medium grained granodiorite from the southern tail of the batholith gives a nine point isochron with an age of 150 ± 9 Ma and an initial $^{87}\text{Sr}/^{86}\text{Sr}$ ratio of 0.7067 ± 0.0002 , although as presented at the GAC spring meeting, 1979, this isochron appeared to be more of a scatterchron than is apparent from the stated errors. Samples from the Mount Carlyle Stock, in the east of the region studied, gave an age consistent with the previous K/Ar date of 164 Ma. It is postulated that these Jurassic plutonic rocks experienced reheating and deformation at later times up to the Eocene producing much of the ambiguity in previously published K/Ar data.

2.2 Petrology

The rocks of the northwestern region of the Nelson batholith may be divided into three main groups: the main body of the batholith, composed predominantly of a massive medium to coarse grained granodiorite (Plate I [1]), a more mafic, quantitatively minor, border phase (Plate II [1]) and numerous porphyritic satellite bodies (Plate I [3]) which intrude the sediments to the north of the batholith. In addition small dioritic xenoliths (Plate II [3]) were found within the main body of the granodiorite. Approximate modal analyses and norms for the twenty-four samples which

Plate I

- 1 Main body granodiorite, hand specimen
- 2 Main body granadiorite, thin section
- 3 Porphyry, hand specimen
- 4 Porphyry, thin section

PLATE I

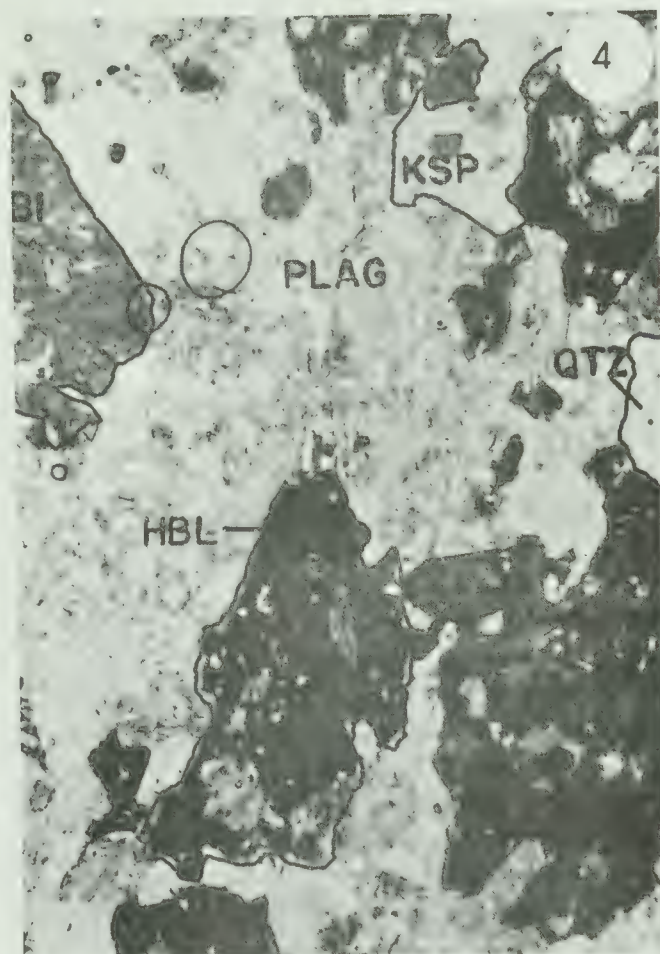
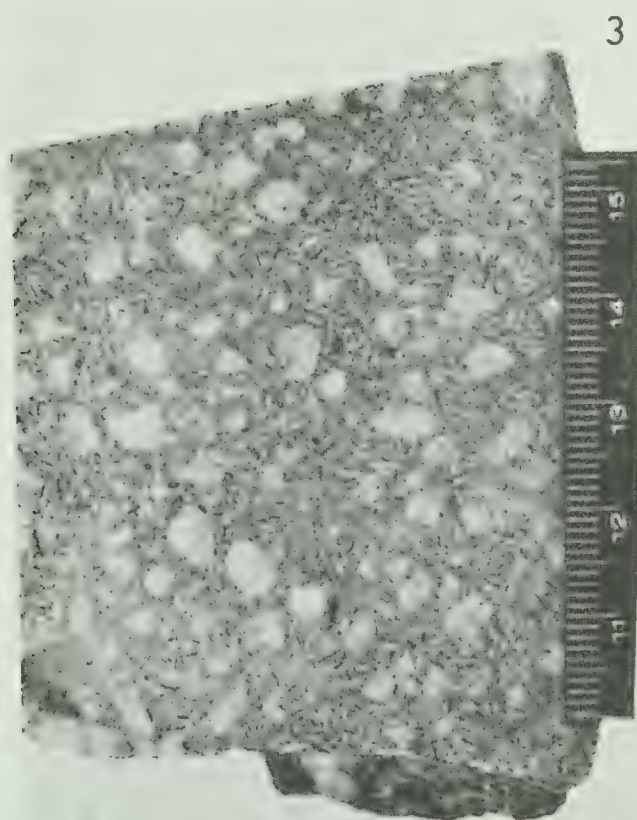
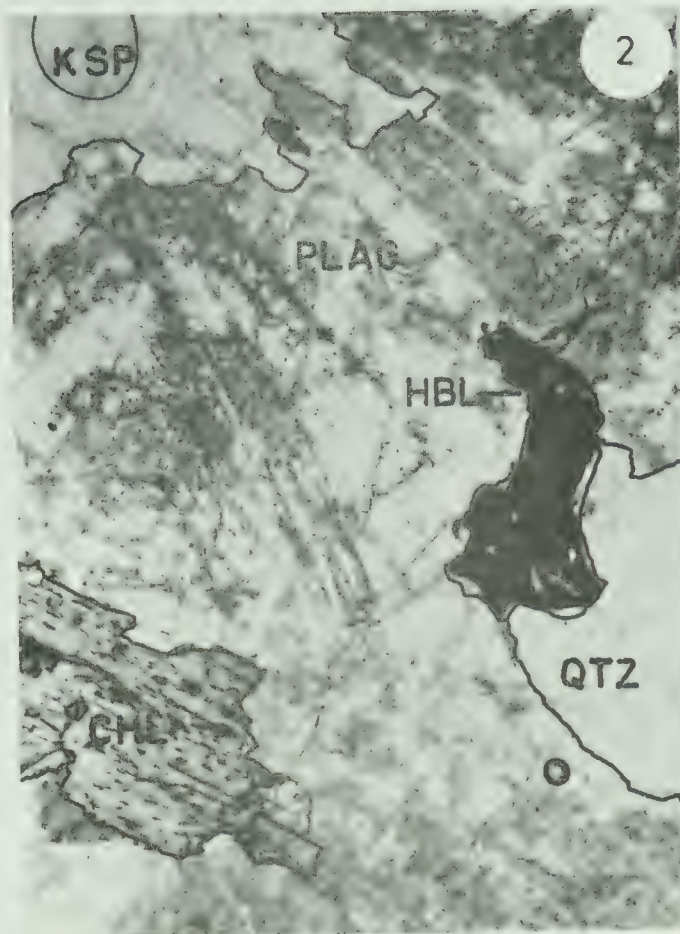
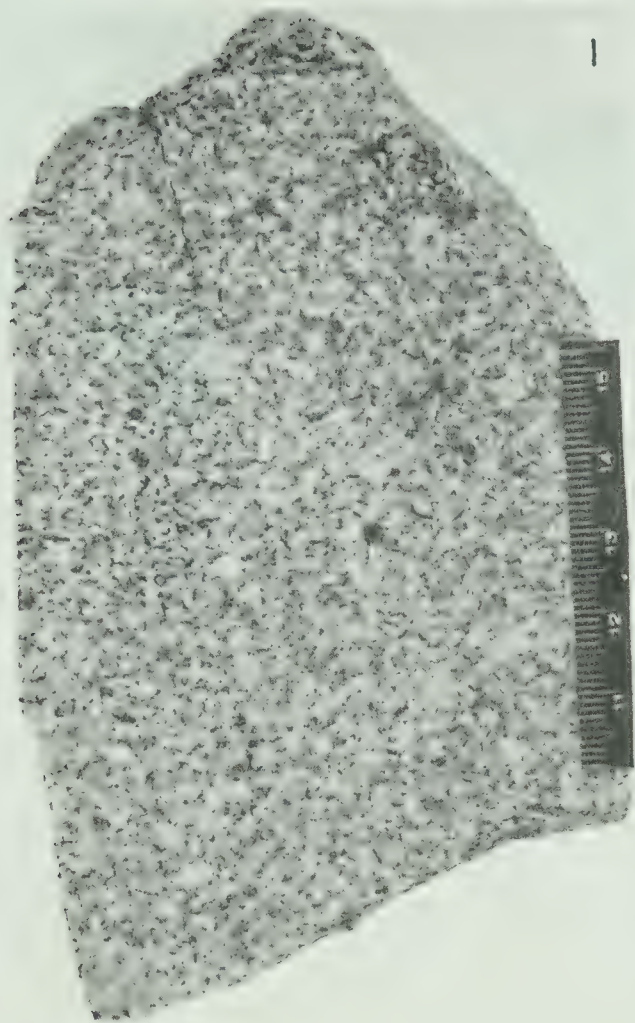
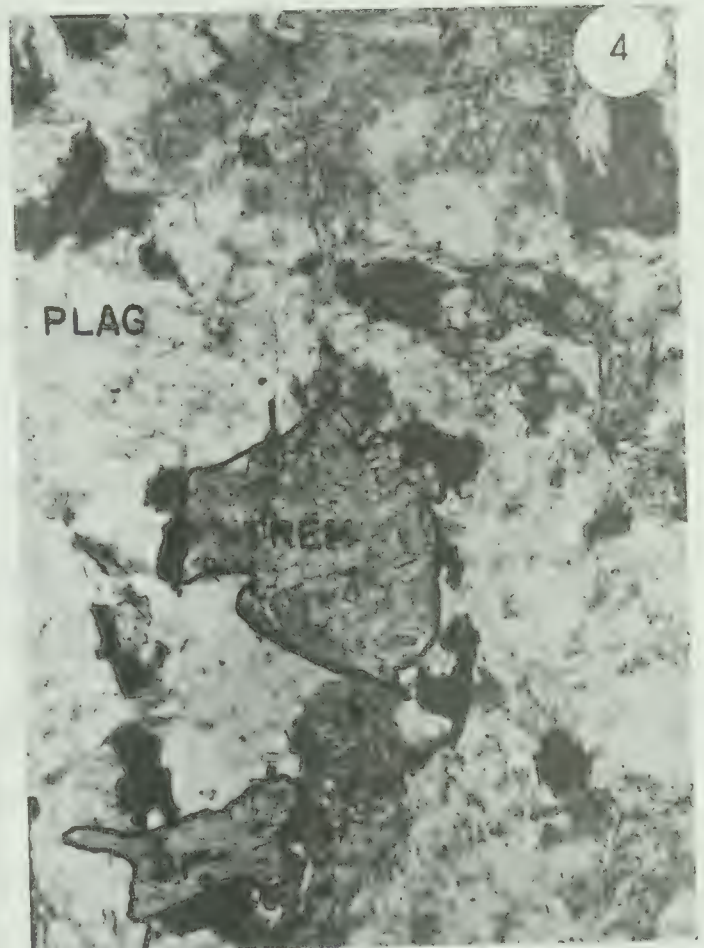
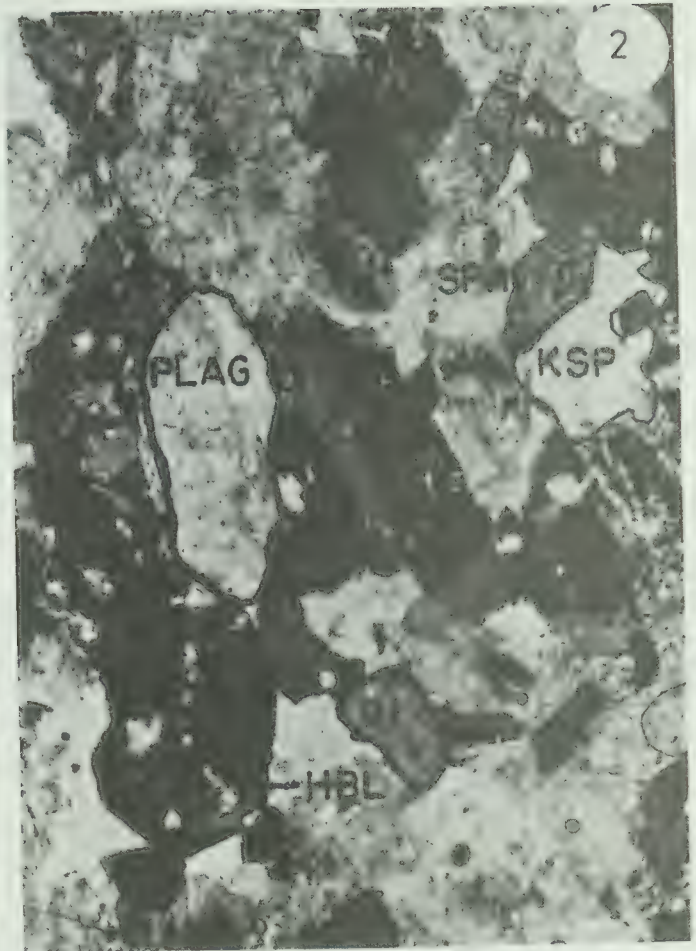


Plate II

- 1 Border rock, hand specimen
- 2 Border rock, thin section
- 3 Xenolith, hand specimen
- 4 Xenolith, thin section

PLATE II



were analysed for major and trace elements are given in Appendix 1.

In thin section the main body rocks (Plate I [2]) display a coarse intergrowth of euhedral plagioclase feldspar, ranging in composition from An_{26} to An_{32} and commonly showing zoning, anhedral K-feldspar and quartz. Subhedral hornblende predominates over biotite as the major mafic mineral and these account for around 10% of the rock. Accessory minerals are euhedral sphene and opaque oxides. In composition the rocks group close to the granodiorite/quartz monzodiorite/quartz monzonite boundary on the Streckeisen classification with the majority falling in the granodiorite field. Sample 7.16 contains only very minor mafic minerals and classes as a hololeucocratic granite.

The border rocks become increasingly mafic towards the margin of the batholith. Large euhedral plagioclase feldspar of composition An_{35} is the major felsic mineral with interstitial K-feldspar and less than 5% fine grained quartz (Plate II [2]). Hornblende composes up to 35% of the rock and sphene and opaque oxides are again the accessory minerals. The border rocks classify in the monzonite-monzodiorite range.

All the satellite porphyry bodies contain large euhedral plagioclase phenocrysts of composition An_{25} to An_{30} , many showing strong zoning (Plate I [4]). Quartz appears in two distinct phases; as occasional large euhedral crystals and as a component of a fine grained quartz/feldspar late stage matrix. Euhedral hornblende and biotite account for 10-20% of the rock. The modal compositions of the porphyries range from granadiorite to quartz monzodiorite.

Evidence of late stage hydrothermal alteration is found in almost all the rock samples from the Nelson batholith. Sericitization of the plagioclase feldspar is widespread, and dark grey patches of epidote are also

found on the plagioclase crystals. It is believed that the Ca needed to produce epidote is released by the feldspar as it absorbs Na from the hydrothermal solutions. The mafic minerals are also often altered. Biotite may be almost completely replaced by chlorite and epidote is found in many samples in association with chlorite and appears to be forming at the expense of hornblende.

The samples from the xenolith are distinct from the rest of the igneous rocks. These porphyritic medium grained rocks do not show normal igneous textures (Plate II [4]); the plagioclase feldspar is highly zoned and the crystals have corroded margins, indicating a non-equilibrium assemblage. The amphibole is tremolite/actinolite and it appears to pseudomorph relic pyroxene crystals. Biotite is less prevalent than amphibole and there are very few opaque minerals in this rock type which classifies in the monzonite/monzodiorite range.

In conclusion, the field relationships and petrological evidence suggest that the border rocks were the initial differentiates of the crystallising magma which were pushed to the margins as the main granodioritic mass was emplaced. The porphyries have a range in composition and do not all appear to have been intruded at the same time but may be characterised by relatively rapid movements of magma from depth to the final position of emplacement. The xenolith samples have a different origin from the rest of the intrusives; further discussion on this topic will be delayed until the geochemistry of the rocks has been considered. Hydrothermal alteration of the northwestern section of the Nelson batholith appears widespread.

2.3 Geochemistry of the Nelson Batholith

The major and trace element analyses of the igneous rock samples are shown in Appendix 1.

(i) Major elements

Compared to the average granodiorite (Nockolds 1954) the rocks from the main body of the batholith are high in Al, Fe, Ca, Na and K. On an AFM plot (Figure 5) they fall on a typical calc-alkaline differentiation trend with the border rocks showing higher Mg and Fe, typical of early differentiates from a crystallising magma. Sample 7.16 is a very late differentiate and stands out on all the chemical variation diagrams. On both the AFM and the MgO vs. SiO_2 (Figure 6) diagrams the porphyries plot along the main trend indicating that differentiation was controlled by the crystallisation of the same minerals as in the main body of the batholith. The xenolith samples fall well away from the calc-alkaline trend and are distinguished by exceptionally high magnesium values.

Average values for the Rossland Group volcanics (Beddoe-Stephens 1977) are also shown on Figures 5 and 6. They plot at the 'early differentiate' end of the calc-alkaline trend.

(ii) Trace elements

The trace element concentrations give clues to the source and cooling history of the batholith. Very low Ni values in all but the xenolith samples are evidence against a simple mixing model involving a large proportion of basaltic magma for the origin of these calc-alkaline rocks.

V/Ni ratios (Figure 7) are high (> 10) which is typical for calc-alkaline rocks (Taylor et al 1969). The V content is similar to that of tholeiitic and alkali basalts whilst the Ni content is an order of

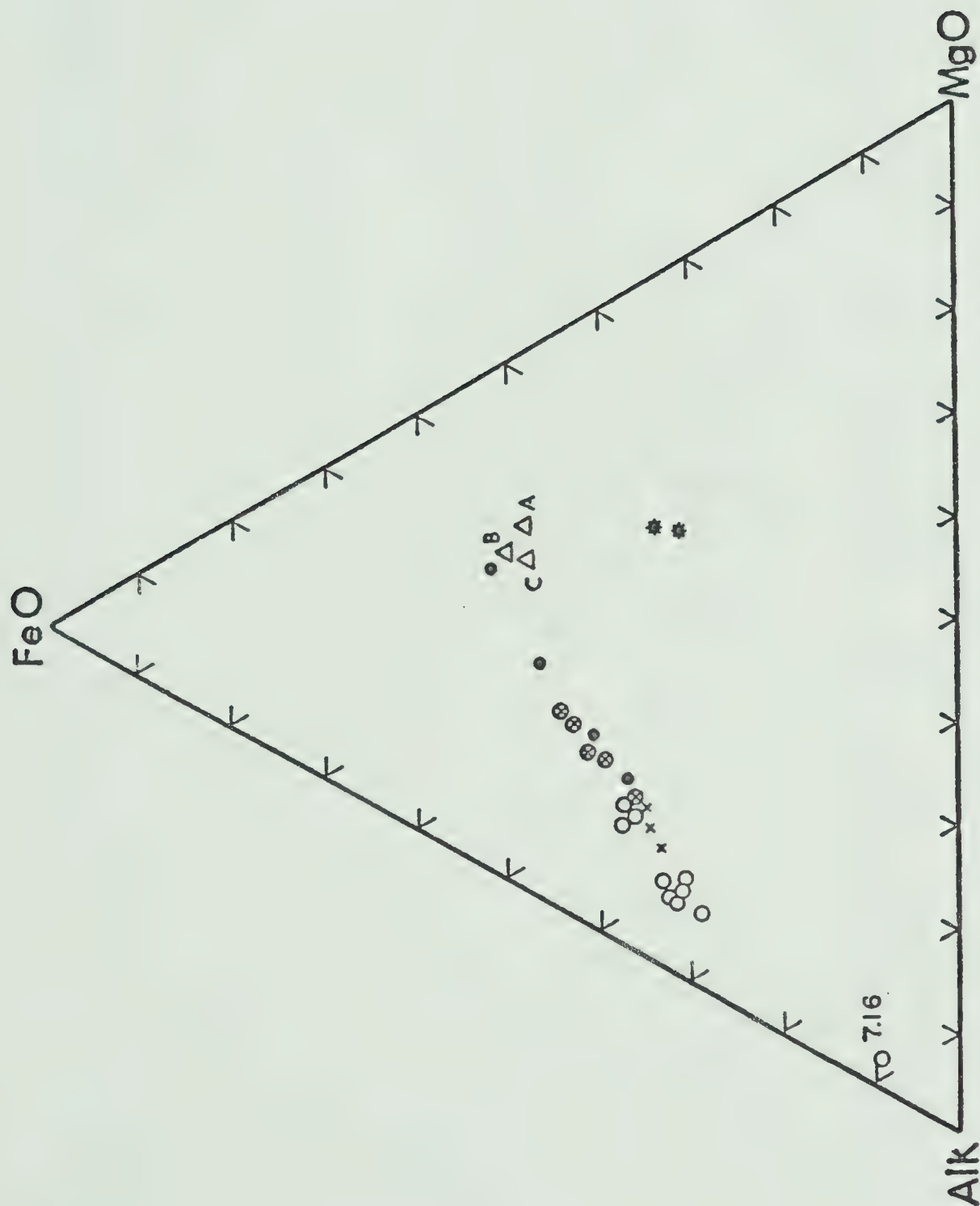
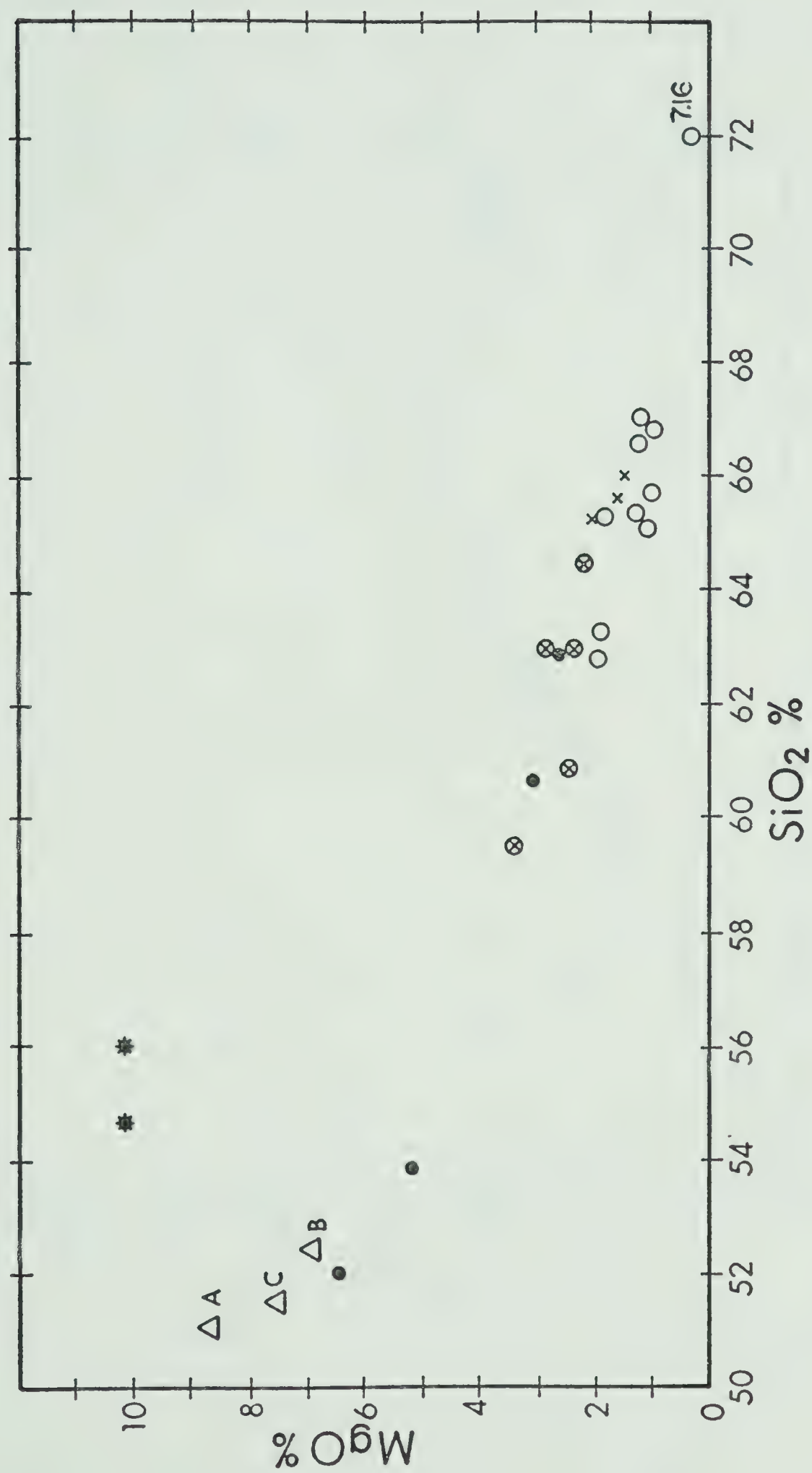


Figure 5. AFM diagram. \circ are from the main body of the batholith; \times are from high (approximately 65% SiO_2) and lower SiO_2 porphyry bodies; \bullet are from border rocks; $\#$ are xenolith samples. $\Delta A, \Delta B, \Delta C$ are averages for the Rossland Group volcanics (Beddoe-Stephens 1977).

Figure 6. MgO versus SiO₂ diagram (symbols as in Figure 5).

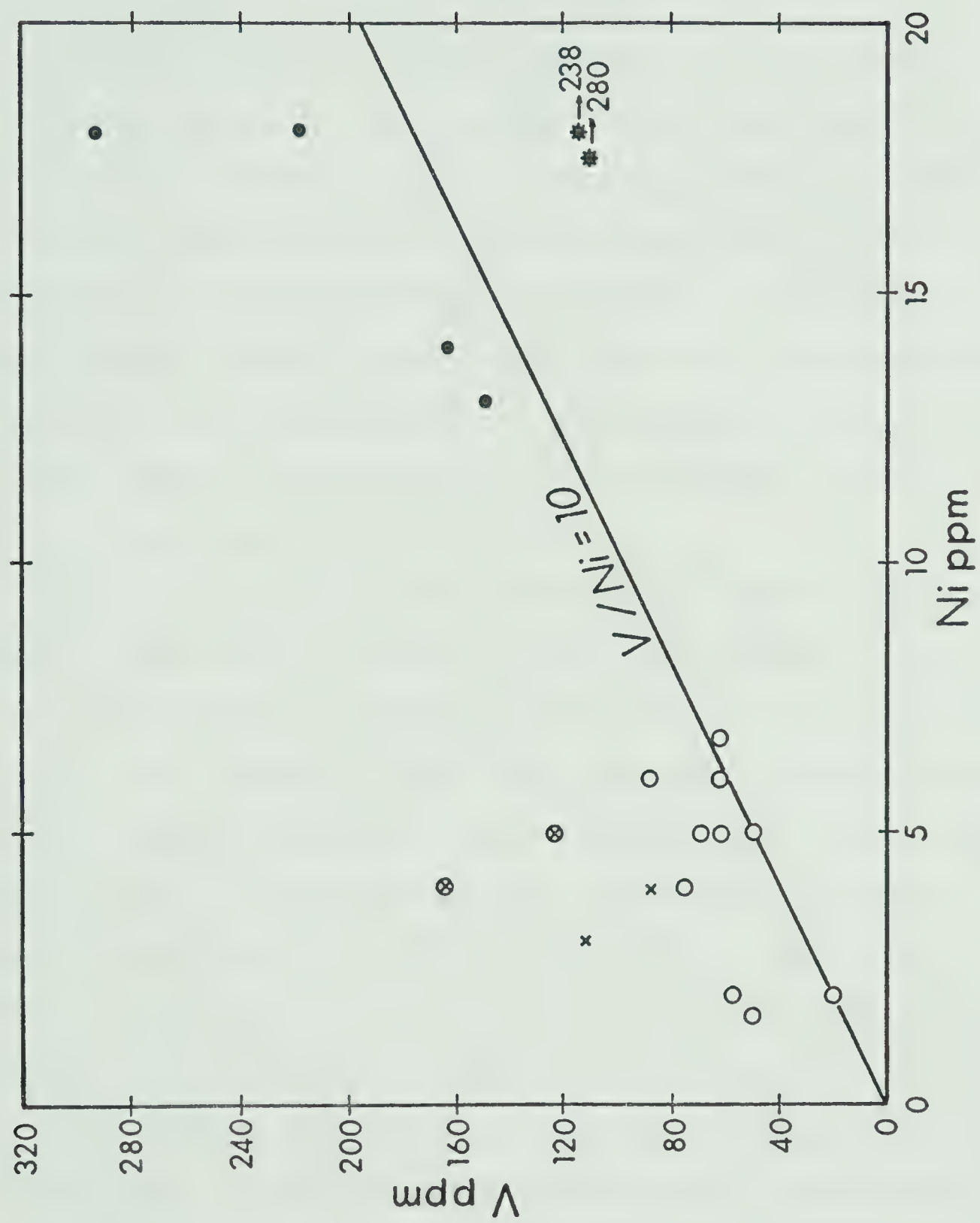


Figure 7. V versus Ni diagram (symbols as in Figure 5).

magnitude lower. This precludes derivation of the batholith from an alkali basalt or tholeiitic basalt by crystal fractionation because V as well as Ni would be depleted in the residual magma.

Rb has the same ionic charge as K but has a larger ionic radius, 1.47\AA compared to 1.33\AA . During magmatic crystallisation Rb will be admitted by K and therefore K/Rb ratios would be expected to be highest in the early fractionating rocks. Figure 8 shows that all the border rocks have K/Rb ratios greater than 330 whilst all the main body batholith rocks, except for sample 7.16, have K/Rb ratios below 330 consistent with the theory that fractional crystallisation of the magma took place. The high K/Rb values of the porphyries are similar to those of circum-Pacific igneous rocks (Taylor et al 1969).

Although the porphyry bodies follow the main batholith trend with regard to major element variation they may be distinguished by their trace element concentrations. They have high V/Ni and K/Rb ratios and have low Nb, Y and Zr contents. On the TiO_2 vs FeO (Total) diagram (Figure 9) the main body and border rocks show a remarkably linear trend but the porphyries fall on a separate line showing lower Ti concentrations. This suggests that the porphyries did not simply form from rapidly rising offshoots of the main Nelson magma chamber. The lack of field relationships make it difficult to tell whether the porphyries pre-date or post-date the main Nelson batholith but it seems that they were derived from a similar magma, but one having higher K/Rb and V/Ni ratios and lower concentrations of Nb, Y, Zr, and Ti than the main Nelson magma. The porphyries indicate that at least two phases of magma genesis occurred in the region. It is interesting to note that the Rossland Group volcanics plot on the extension of the porphyry trend, possibly reflecting

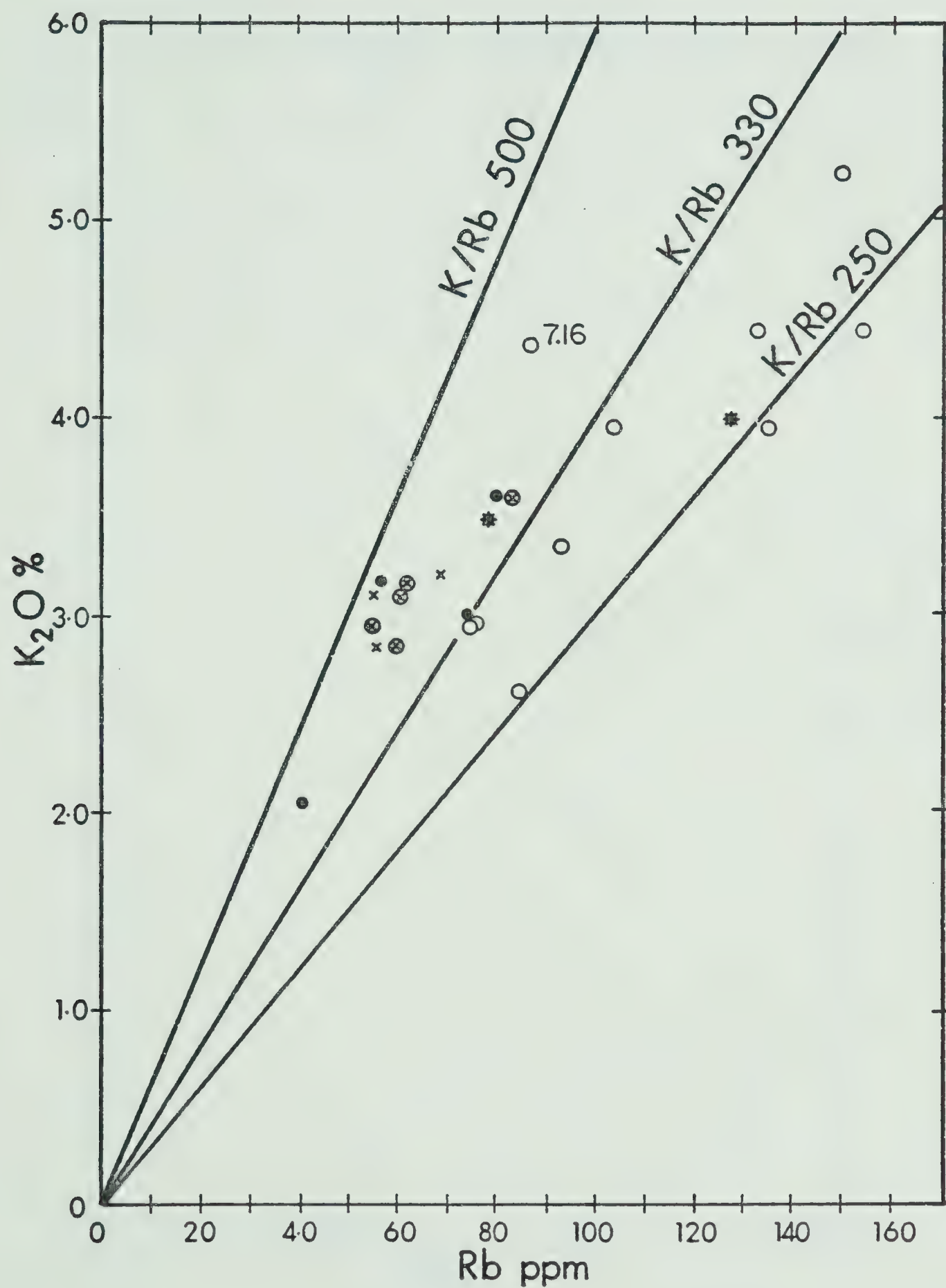
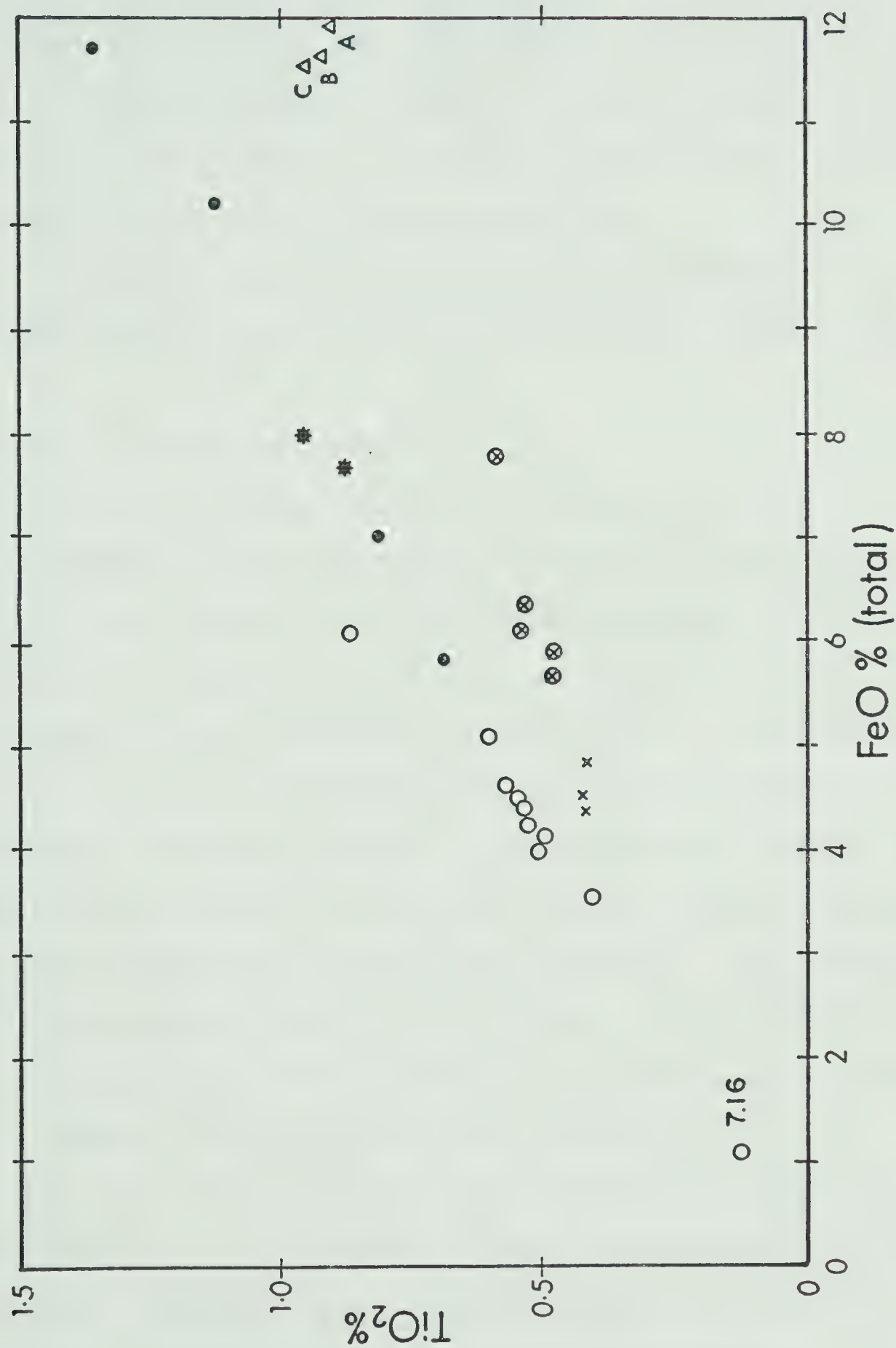


Figure 8. K_2O versus Rb diagram (symbols as in Figure 5).



a comagmatic relationship between the two.

Figures 10 and 11 show that the positive correlation between V and FeO (Total) and V and MgO. The early differentiates are high in V compared to the main body granodiorites as V follows Fe and Mg in the early crystallising mafic minerals. The porphyry bodies and the Rossland volcanics fall along the main differentiation trend.

The distinctive feature of the trace element geochemistry of the xenolith samples is the exceptionally high Ni and Cr concentrations.

2.4 Origin of the Nelson batholith

The nature of granitoid magma is such that it is thought that it may be produced by either differentiation or partial melting processes. The long-lasting debate on this subject has been recently sharpened by the grouping of granitoids into I-types of igneous origin, and S-types of sedimentary origin, by Chappell and White (1974). This division is based partly on the relatively low Na and high Al of S-types reflected by more than 1% normative corundum. Mineralogically this means S-types never contain hornblende. In addition S-type granitoids are restricted to relatively high SiO₂ contents, greater than 69.5% SiO₂ (Chappell 1978), whereas many I-types are less siliceous. Initial ⁸⁷Sr/⁸⁶Sr ratios also show systematic differences with S-types commonly having initial ratios greater than 0.710 (Chappell and White 1974).

The rocks of the northwest margin of the Nelson batholith show a wide range in silica content with only one sample containing more than 69.5% SiO₂. Corundum is only present in the norm of one out of twenty-four samples and hornblende is the most abundant mafic mineral. These factors all point to an igneous origin for the Nelson batholith. Whole

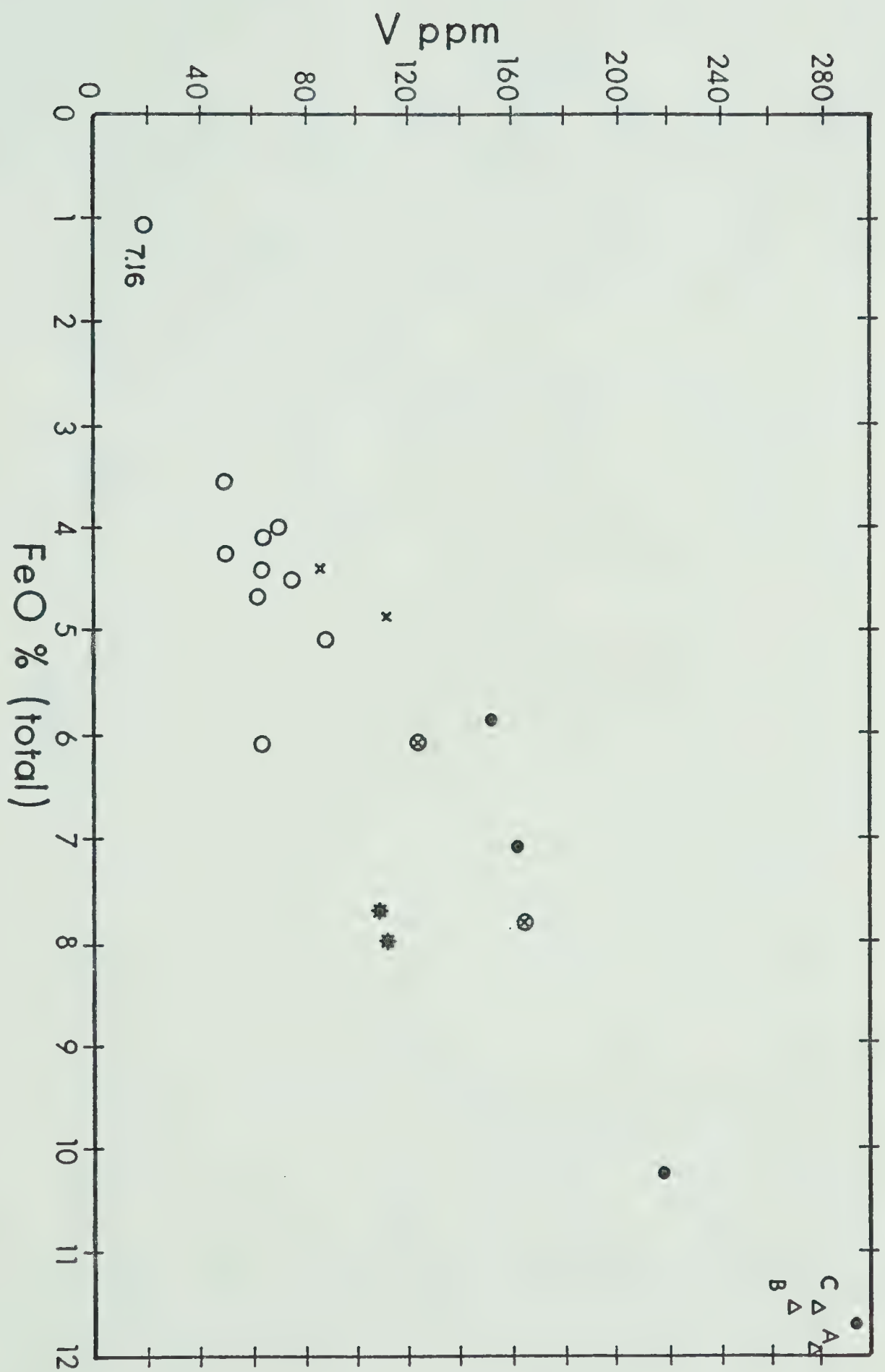


Figure 10. FeO (total) versus V diagram (symbols as in Figure 5).

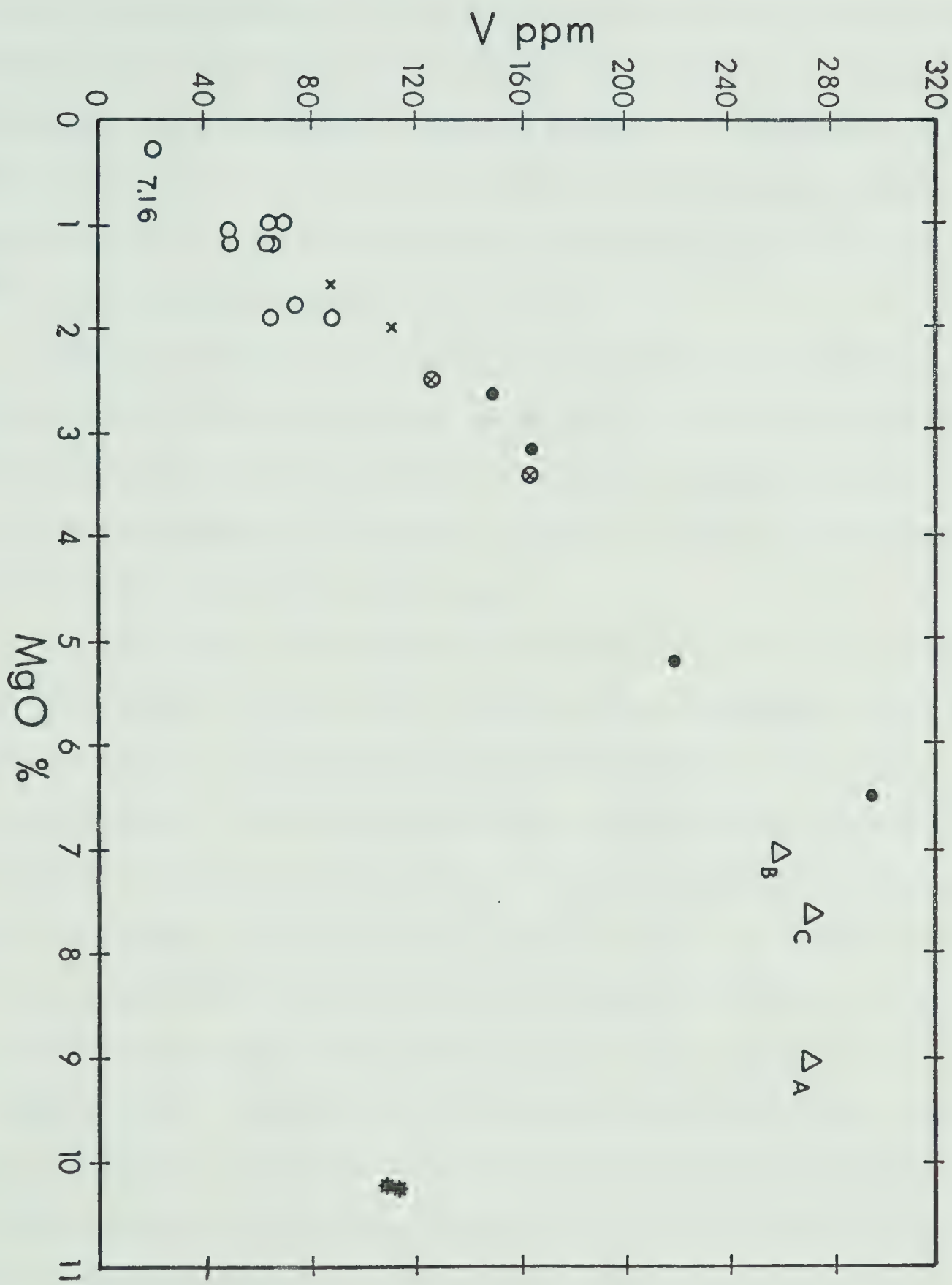


Figure 11. MgO versus V diagram (symbols as in Figure 5).

rock initial $^{87}\text{Sr}/^{86}\text{Sr}$ ratios of approximately 0.707 fall well below the higher values associated with continental crustal rocks (Fairbairn et al 1964, Duncan et al 1979) which rules out the possibility of large scale selective fusion of ancient or Rb-rich geosynclinal sediments as the batholith source. The low values indicate that the magma originated in the base of the crust or upper mantle and became slightly enriched in ^{87}Sr as it migrated upwards.

There is evidence in the paragneisses in the core of the batholith, to the south of the mapped area, that parts of the batholith were formed by the metasomatism of pre-existing sediments. However, it seems probable that these paragneisses are merely remnants of relatively minor volumes of sediments 'digested' by the magma.

In conclusion, the geochemistry and petrology of the rocks from the northwest region of the Nelson batholith indicate that they formed by differentiation, controlled by crystal fractionation, from a calc-alkaline magma. The origin of such calc-alkaline magmas has been widely discussed in geological literature. Their close spatial association with island arcs the low initial $^{87}\text{Sr}/^{86}\text{Sr}$ ratios and results of high pressure experimental studies (Green and Ringwood 1968) have led to the belief that the magmas have formed by a two stage process from the mantle (Ringwood 1974). Oceanic crust is generated from the primitive mantle at an ocean ridge. As part of the lithosphere it moves down into the mantle along a subduction zone where, at depths of 70-100 km, amphibolite in the crust becomes dehydrated and the water generated causes partial melting of the pyrolite upper mantle adjacent to the subduction zone. These magmas differentiate to give the early tholeiitic stage of island arc development. At depths of 100-150 km a high partial pressure of

water is maintained in the oceanic crust by the dehydration of serpentine. Partial melting produces magmas which react with the overlying mantle resulting in the formation of low viscosity diapirs which rise upwards from the subduction zone. The diapirs partially melt to give the magmas which fractionate by amphibole crystallisation to produce the calc-alkaline phase of island arc development.

The xenolith, with high MgO, Ni and Cr concentrations, is perhaps a remnant of the refractory material which was not melted when the granitoid magma formed. Such refractory components, carried upwards by the magma, have been termed 'restites' by White and Chappell (1977).

CHAPTER 3

THE SLOCAN GROUP

3.1 Introduction

The Slocan Group sediments are exposed to the north of the Nelson batholith. They are, for the most part, a sequence of grey to black, massive, argillaceous sediments apparently deposited by distal turbidity currents with minor slaty, calcareous and quartzitic horizons. The thickness of the Group has been the subject of debate. Cairnes (1934) gave an estimate of 2100 m but Hedley (1952) and Irwin (1951) proposed much greater thicknesses, the latter suggesting around 11000 m. Cairnes (Irwin 1952) objected to this figure on the grounds that major repetitions of strata had been missed. The author, during his field studies, noted numerous reversals of dip from the general southwesterly direction but these appeared due to minor scale folding. It seems that the total thickness of the Slocan Group is very great but an accurate figure may not be placed on it at the present time.

Fossil evidence for the age of the Slocan Group is not conclusive. It appears that the lower part of the Group is almost certainly of Triassic age, whilst the upper part of the Group is given as provisional Sinemurian (early Lower Jurassic) age. This does not conflict with the K-Ar isotopic age date of 171 Ma (Gabrielse and Reesor 1964), for the initial phase of the Nelson batholith which intrudes the sediments.

Cross bedding, graded bedding and soft sediment deformation structures were seen in the turbidites throughout the sequence. The basal beds

in the northeast of the mapped area were more fissile and calcareous than beds higher in the sequence where, to the southwest of Sandon, numerous quartzitic horizons were noted. The highest beds of the Slocan Group outcrop towards Slocan Lake and the Nelson batholith contact. They are again predominantly argillaceous but contain minor beds of tuffaceous origin.

The structure of the Slocan Group has been discussed in detail by Hedley (1952). The dominant feature is a large recumbant syncline termed the 'Slocan fold' by Hedley. This is exposed along a 20 km section trending northeast and southeast from Sandon. Strata in the valleys dips southwest; at moderate elevation the dip is vertical whilst on the peaks the dip is northeast and the strata are overturned. The beds thus form a recumbent syncline with associated local crumpling folds and faults of small displacement.

The grade of regional metamorphism in the area is not as high as that in the Kootenay Arc to the east. Chlorite and biotite are found in argillites well away from the contact aureole of the Nelson batholith indicating low grade regional metamorphism. Within around 800 m of the main batholith contact, the metasediments have been partly recrystallised and the development of a wide variety of metamorphic minerals reflects the varied composition of the Slocan sediments. Tremolite was found in more calcareous rich horizons at distances ranging from 100 m to 700 m from the batholith contact. Actinolite was identified in a sample approximately 300 m from the contact whilst garnet, staurolite and biotite were found in an argillite from 2 km east of Fish Lake, well north of the main batholith, indicating the proximity of a satellite porphyry body. Contact aureoles around the porphyry bodies are dependent on the size of

the intrusion. Anthophyllite and cordierite were found in a metasediment approximately 30 m from the edge of the porphyry found east of New Denver, from which sample 7.18 was taken.

3.2 Sampling

Groups of twenty samples were taken from well exposed sections in the Slocan Group sediments. Five groups were collected and their locations are shown as B1, B2, B3, B4 and B5 on Figure 4. Samples of B1 were collected at 6 m intervals from a continuous section of argillites striking at 320° and dipping steeply to the southwest. Within the group, significant compositional variation is found, which is typical of all five groups. Thin section studies showed angular to sub-angular detrital quartz and plagioclase feldspar grains, less than 0.2 mm in diameter, with minor chlorite and iron oxides in a very fine grained matrix. Calcite appeared to be recrystallising in the sediment.

B2 samples were taken at 4 m intervals from a section very close to the top of the Slocan Group and had the same dip and strike as the B1 group. In thin section an argillite sample showed an interlocking aggregate of detrital angular plagioclase feldspar and quartz grains. Maximum grain size is less than 0.25 mm and this makes positive distinctions between quartz and untwinned plagioclase feldspar difficult. In view of the chemical analyses of the group it appears likely that most of the grains are plagioclase feldspar. Small green crystals of actinolite make up around 10% of the rock reflecting proximity to the batholith and minor biotite, calcite and opaque oxides were identified. Group B2 had the lowest carbonaceous material content of the sediments sampled followed by group B1. Groups B3, B4, and B5 had relatively higher car-

bonaceous contents.

Group B3 samples were taken from a continuous 100 m section south of New Denver, lower down the Slocan Group than groups B1 and B2 but showing the same general dip and strike directions. In thin section a B3 argillite was made up of angular to sub-angular detrital quartz and feldspar grains, diameter less than 0.20 mm, opaque oxides, biotite and minor detrital calcite in a very fine quartz-mica-carbonaceous material matrix. Chemical analysis suggests that most of the detrital grains are quartz.

Group B4 samples were taken at 3 m intervals from a section of argillites northwest of Sardon striking at 310° with an approximate dip of 50° to the northeast. Thin section studies show detrital subangular quartz grains, less than 0.25 mm in diameter, in a very fine grained micaceous matrix. Biotite rich and carbonaceous rich bands were evident along with minor iron/titanium oxides.

Group B5 samples were taken from a 60 m section east of New Denver where the Slocan sediments strike at 340° and dip 38° to the southeast. The position of this section near to a satellite porphyritic igneous intrusion was reflected in thin section by the presence of porphyroblastic needles of anthophyllite and xenoblastic cordierite in a very fine grained quartz/ feldspar/graphitic matrix.

The typical mineral assemblages for the five groups are given in Appendix 2.

3.3 Chemistry and Provenance

Major and trace element analyses were determined for each sedimentary sample and the results are shown in Appendix 2. Average concentrations for each element in each group were calculated after discarding four B1,

three B2, two B3 and four B5 samples due to exceptionally high CaO and MgO percentages. These averages are shown in Table 1. Factor analysis techniques were used to give a general picture of the chemical character of the sediments.

The principal aim in factor analysis is to reduce an observed set of relationships between many variables, in this case the chemical data on the sediments, to a simpler set of relationships amongst fewer variables which may be termed factors. In simple terms, without becoming involved in the mathematics of the method, the factor scores, represented by one point per sample on the diagram (Figure 12), are similar for rocks of similar chemical character. Thus the relative degree of scatter within the sedimentary groups and the relative differences between the groups are displayed.

The principal component matrix factor scores F_1 and F_2 , as displayed in Figure 12, express approximately 70% of the total variance of the data in this example. Groups B2 and B4 are the most different chemically whilst B1, B3 and B5 are intermediate in character with B3 being most similar to B4 and B1 being the most similar to B2. F_1 may be broadly related to $\text{SiO}_2\%$ with positive F_1 samples containing more SiO_2 relative to negative F_2 samples. Similarly F_2 may be broadly related to Rb concentration and $\text{K}_2\text{O}\%$.

The large compositional variation between the Slocan sediment samples is typical for beds deposited by turbidity currents (Condie 1967). This feature can be most readily explained if the turbidity currents were generated from different regions within a partly enclosed basin. The composition of the immediate source area would then determine the composition of the sediment arriving at the edge of the basin. With this factor in

TABLE 1

Average chemical analyses for the Slocan Group sediments

(major elements as weight % oxides, trace elements in ppm)

	B1	B2	B3	B4	B5
SiO ₂	60.7	54.8	74.2	74.0	66.2
Al ₂ O ₃	15.1	14.6	10.4	14.0	13.6
Total Fe as Fe ₂ O ₃	7.6	9.1	3.6	4.2	5.0
MgO	4.2	7.4	1.7	1.2	3.6
CaO	5.0	6.8	4.1	1.0	4.9
Na ₂ O	3.3	3.6	1.9	1.7	2.2
K ₂ O	2.3	1.7	2.5	2.9	2.8
TiO ₂	0.8	0.9	0.6	0.7	0.6
MnO	0.1	0.2	0.1	0.1	0.1
P ₂ O ₅	0.3	0.3	0.2	0.1	0.4
S	0.6	0.2	0.1	0.2	0.7
Pb	32	33	40	33	36
Ba	1517	1222	884	565	1084
Nb	8	6	12	18	14
Zr	90	70	188	240	198
Y	24	19	31	28	38
Sr	462	506	308	242	266
Rb	58	32	65	96	86
Zn	259	112	98	58	255
Cu	74	57	25	23	65
Ni	33	79	22	20	52
Cr	108	235	63	58	116
V	277	189	84	77	276
K/Rb	331	444	316	256	270
Al ₂ O ₃ /Na ₂ O	4.57	4.02	5.44	8.16	6.16

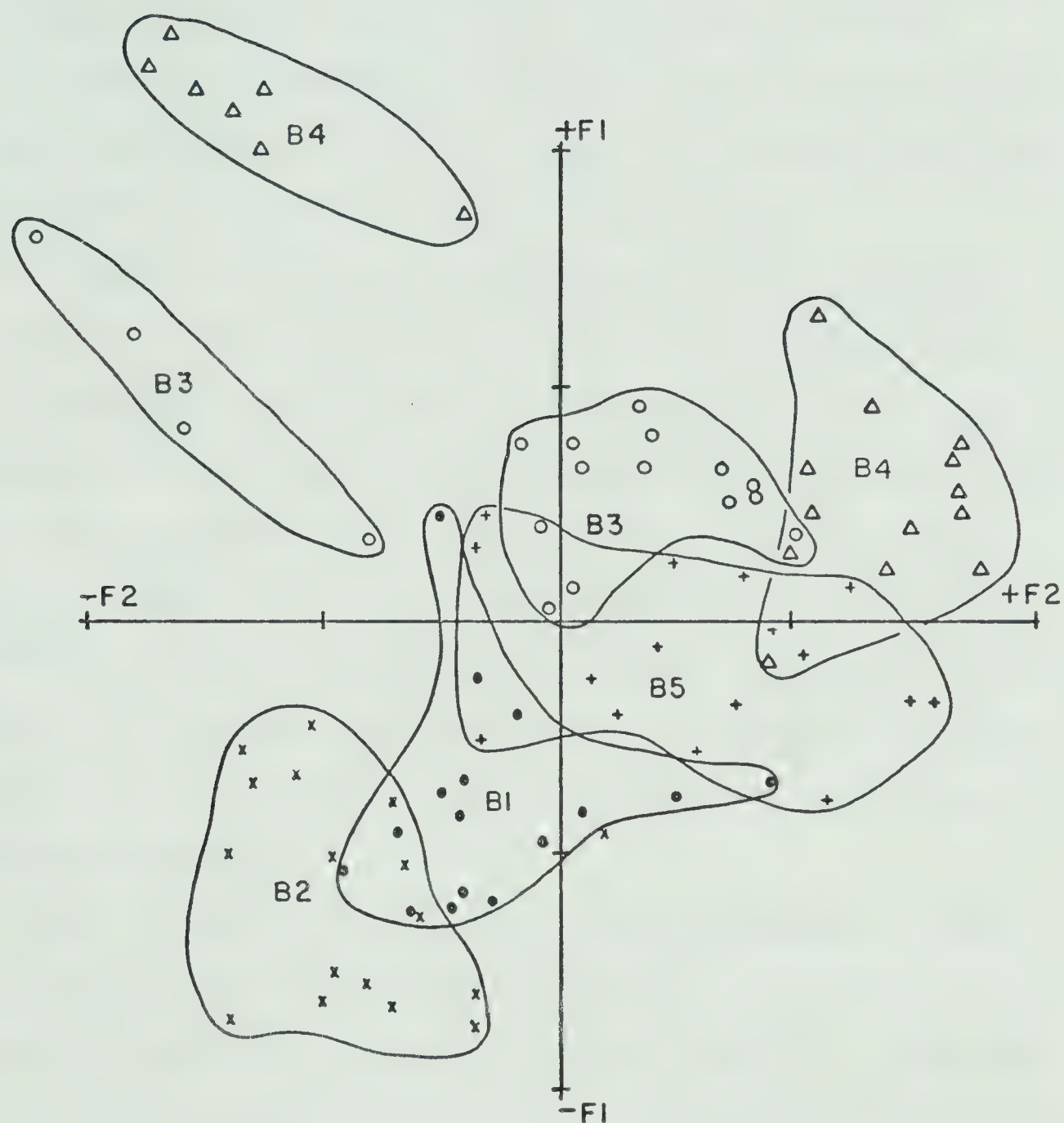


Figure 12. Principal Component Matrix factor scores for groups B1, B2, B3, B4, B5 from the Slocan Group sediments.

mind, and assuming that the low-grade regional metamorphism in the region has been approximately isochemical, a presumption supported by geochemical studies on Californian metagreywackes (Coleman 1965), conclusions may be drawn on the source region of the Slocan Group sediments.

The effect of grain size on the chemistry of the sediments is not considered important as all the groups consist of fine sand-sized grains (less than 0.25 mm diameter) in an argillaceous matrix.

The compositions of the five sedimentary groups are compared to the average values for basic and felsic (granites and granodiorites) rocks; the Rossland Group volcanics (Beddoe-Stephens 1977); the oceanic basalts from DSDP 37, holes 332A, 333 and 334 (Lambert and Holland 1977) and to Upper Palaeozoic oceanic tholeiites from Clearwater, British Columbia (Hall-Beyer 1976). The overall character of the sediments is illustrated in terms of K_2O , Na_2O and CaO and trace elements are used as indicators of provenance. Rb shows the behaviour of the alkali metals, Ti and Zr represent the heavy mineral component and Ni and Cr follow the ferromagnesian minerals.

Figure 13 shows average compositions of the sedimentary groups in terms of K_2O , Na_2O and CaO . B2 plots very near to the field for basic rocks whilst B4 fall in the range of felsic rock types. B1, B3 and B5 are intermediate in composition with B1 having the highest basic component of these three groups.

K/Rb ratios of sediments are controlled by three main factors: the K/Rb ratio of the source region; metasomatic metamorphism of the sediments and the effects of transport and deposition. During transport and deposition Rb may be concentrated relative to K away from the source and so, when comparing sediments showing different K/Rb ratios, the lower

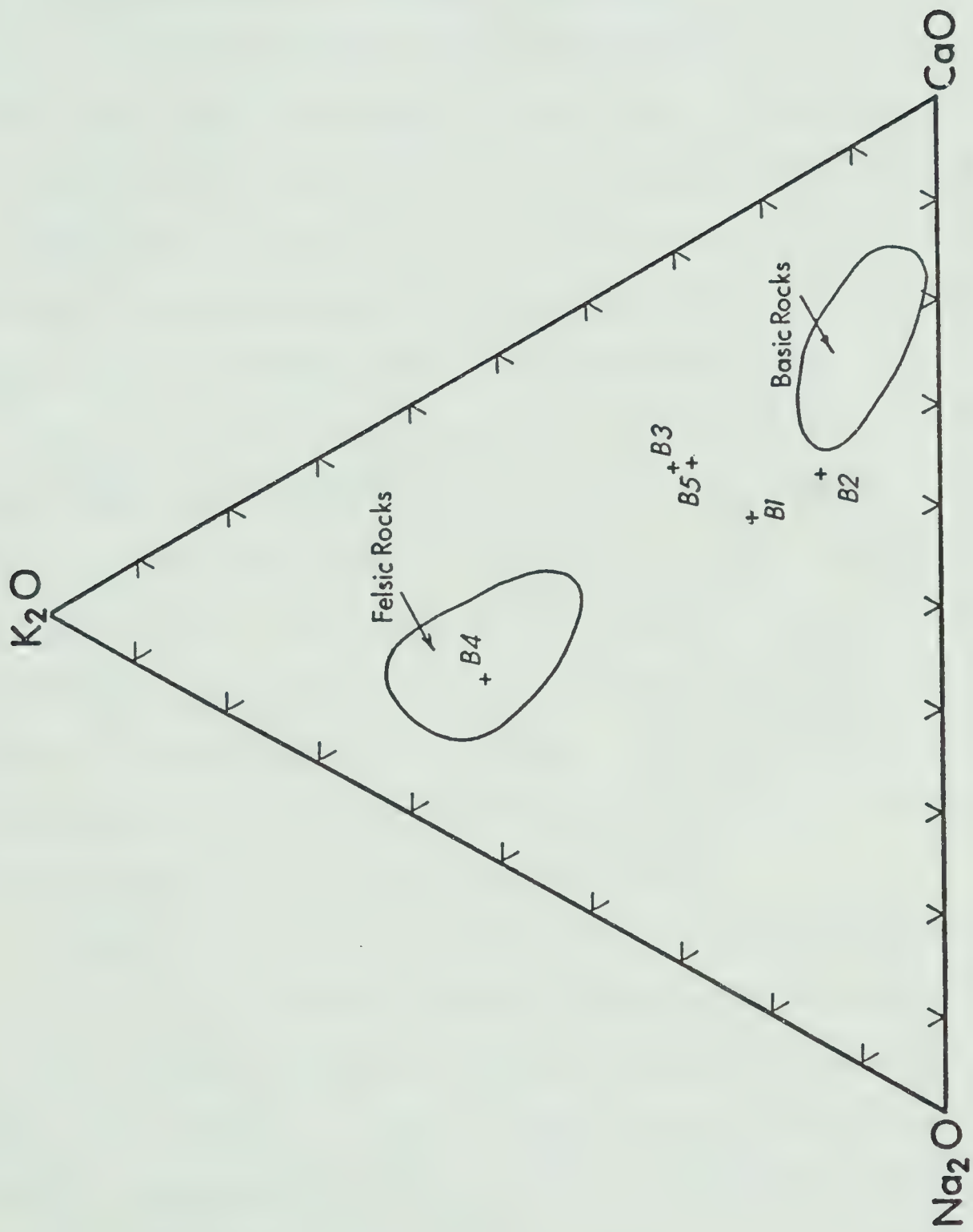


Figure 13. K_2O : Na_2O : CaO diagram for the averages for groups B1, B2, B3, B4 and B5. The fields for felsic and basic rocks from Condie (1967).

ratio may reflect a different source region or merely greater distance from the same source of the sediment with the higher K/Rb ratio. Low grade regional metamorphism does not effect K/Rb ratios but contact metamorphism may concentrate Rb towards the contact. B2 is the group from nearest to the Nelson batholith and has the highest K/Rb ratio (Figure 14) so the effect here is apparently not important. B2 again shows the most basic character followed by B1. B4 plots nearest to the field of granites and granodiorites. There is considerable variation within the groups of both $\text{SiO}_2\%$ and K/Rb values. Despite this there is only minor overlap of the groups and no overlap between B2 and the other groups.

The variation of TiO_2 and Zr for the sediments is shown in Figure 15. These elements are representative of the detrital component of the sediments and reflect the chemistry of the source region. TiO_2/Zr ratios of the groups display a similar geochemical pattern to the previous plots. B2 again has the most basic character followed by B1 whilst B3, B4 and B5 have a much greater felsic component. Once again there is considerable deviation from the average within the groups but no overlap occurs between the basic and the more felsic sediments.

Average Ni and Cr concentrations show a positive and almost identical correlation with MgO (Figures 16 and 17) indicating that these two trace elements are entering the ferromagnesium silicate phase (chlorite) in the sediments. B2 shows a very large variation within the group, Ni and Cr concentrations increase with increasing $\text{MgO}\%$ and decreasing $\text{SiO}_2\%$ and the average for the whole group is typical for that of a basic rock. The other groups show less internal variation: B3 and B4 have concentrations typical of granodiorites whilst B1 and B5 have an intermediate composition. It has been shown by Goldberg and Arrhenius (1958) that

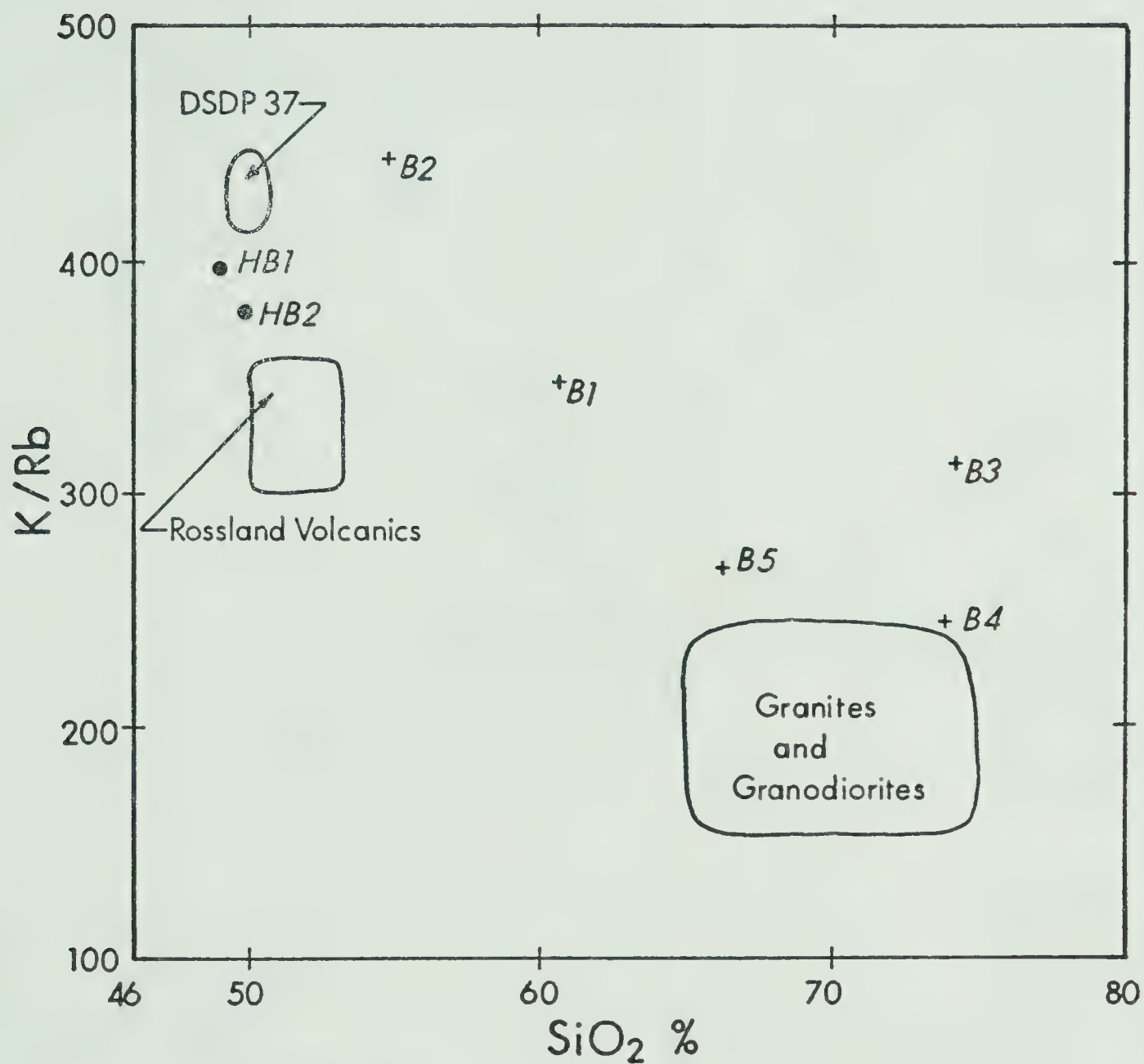


Figure 14. SiO_2 versus K/Rb diagram.

Averages for the Slocan Group sediments are compared to the Rossland volcanics (Beddoe-Stephens 1977); DSDP 37 (Lambert and Holland 1977); HB1 and HB2, averages of high Zr and average Zr oceanic tholeiite suites (Hall-Beyer 1976) and the general field for granites and granodiorites (Condie 1967).

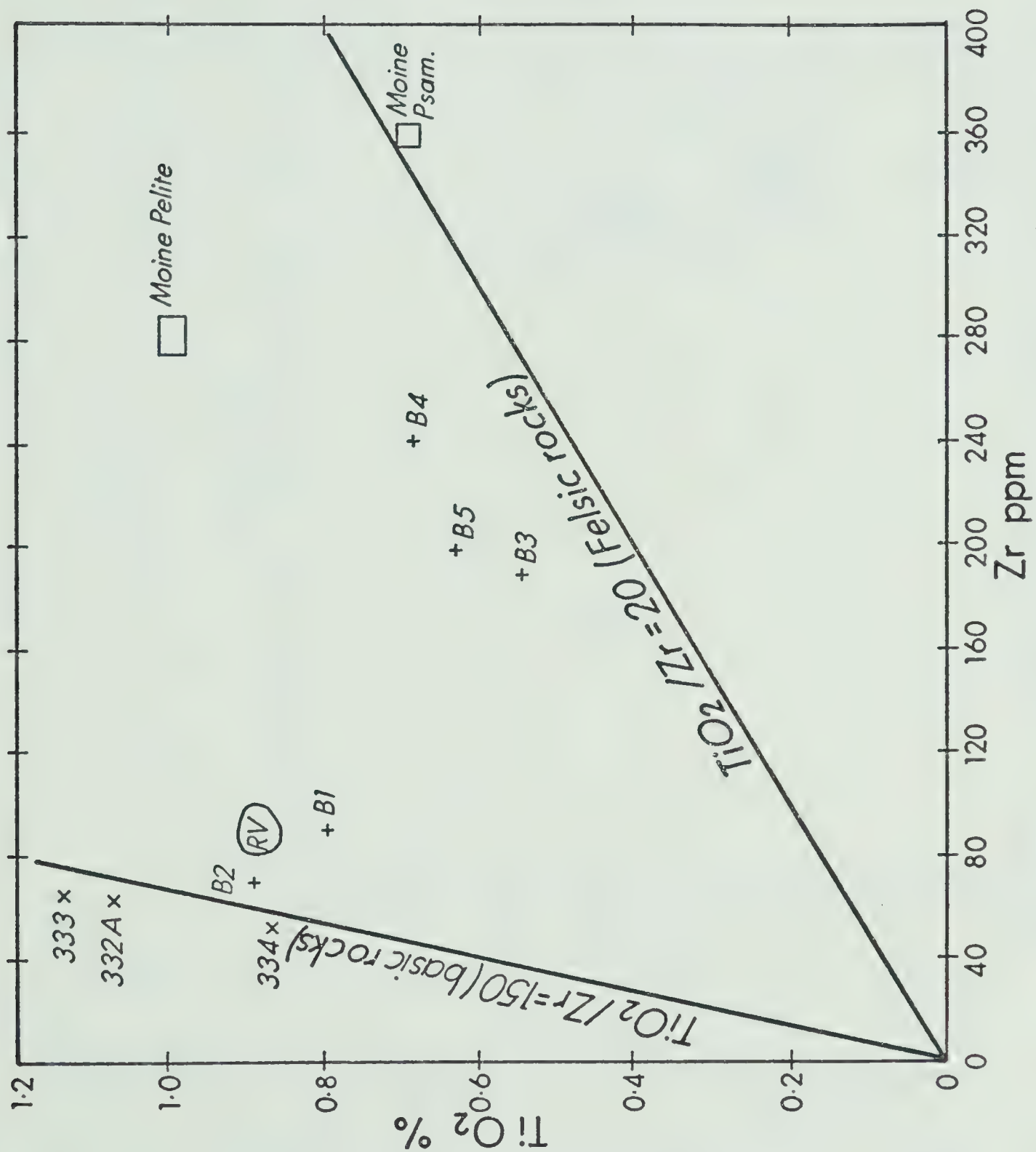


Figure 15. TiO_2 versus Zr diagram. 332A, 333 and 334 are basalts from DSDP 37; RV is the field for the Rossland volcanics; Moine Pelite and Moine Psammite values from Holland and Lambert (Unpublished data)

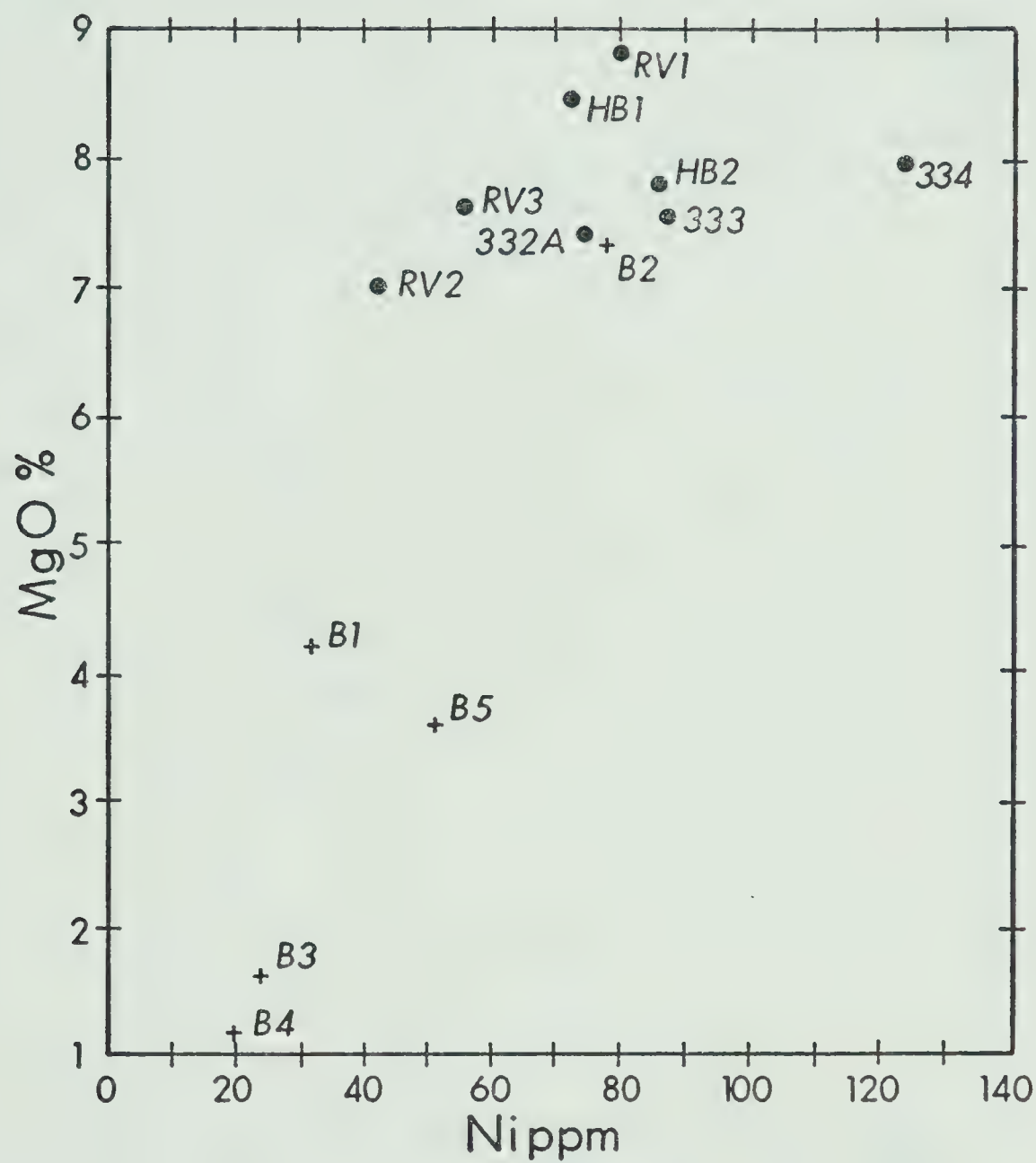


Figure 16. MgO versus Ni diagram (symbols as in Figures 14 and 15).

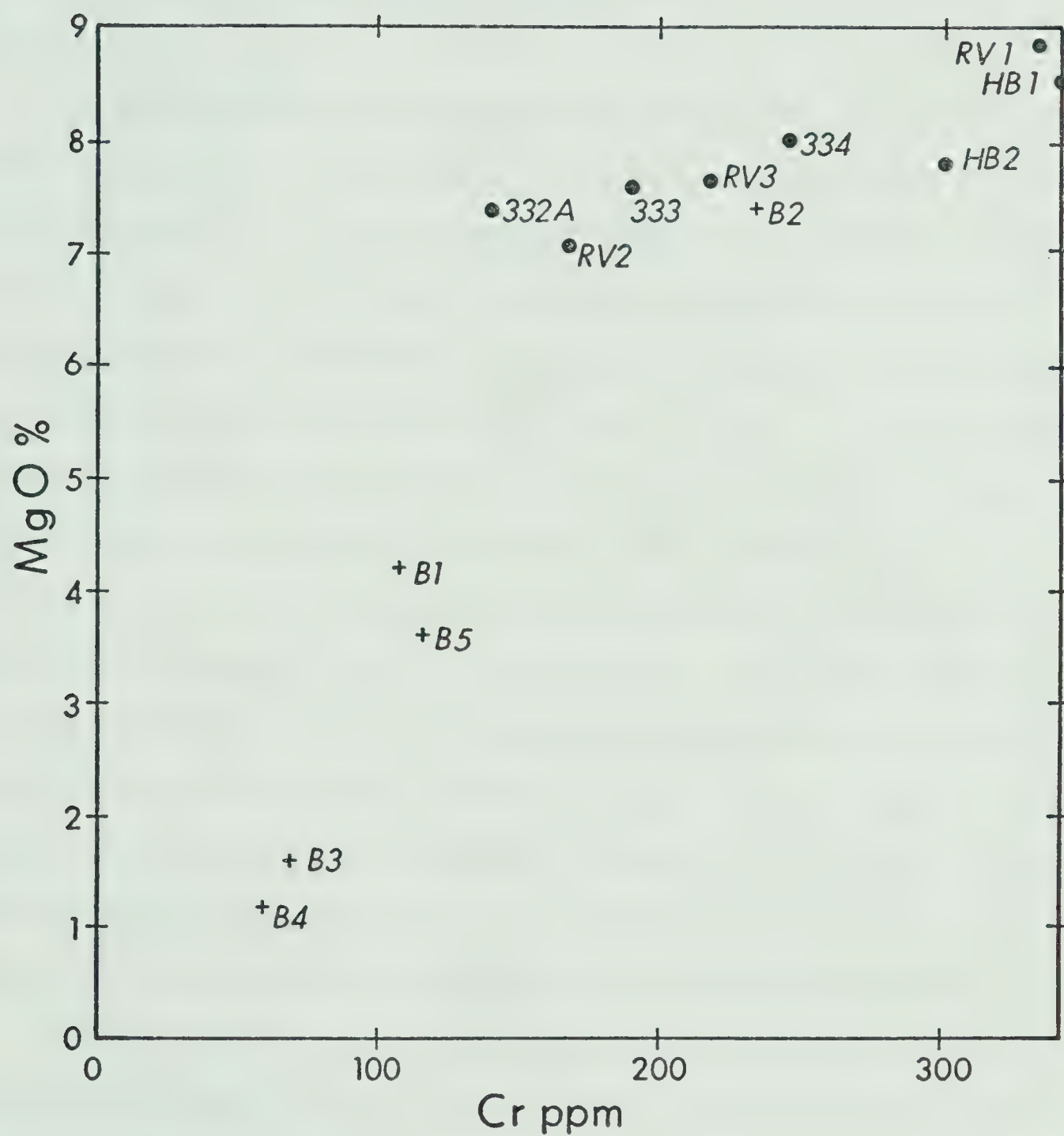


Figure 17. MgO versus Cr diagram (symbols as in Figures 14 and 15).

the concentrations of Ni and Cr in sediments derived from a basic source decrease with distance away from the source region and so the previous results may be explained either by postulating different source regions for the sedimentary groups and/or varying distances from the basic source.

The geochemistry of the Slocan Group gives consistent but not conclusive evidence on the source of the sediments. Any conclusions drawn must be compatible with other geological aspects of the region. Except for in the highest part of the Slocan Group the most common non-argillaceous horizons are calcareous and quartzitic indicating a depositional environment distant from a silica rich source region. In the highest part of the sequence tuffaceous horizons have been found indicative of the relative proximity of volcanic activity. Fossil evidence shows that these beds have a probable Lower Jurassic age which is the period when the Rossland volcanics island arc was emerging. These basic volcanics, or rocks of similar composition, appear to have been the source of the B2 group sediments, the youngest sediments sampled. Slightly lower in the section, the B1 group have a large basic component but also some felsic character possibly because the island arc source region was not fully emerged and was therefore more distant from the depositional basin.

The sediments from lower in the Slocan Group; B3, B4, and B5, are different geochemically from the younger beds. Al_2O_3/Na_2O ratios, suggested by Pettijohn (1957) as a sandstone maturity index, show B4 to be the most mature of the sedimentary groups, a character which is confirmed by the presence of corundum in the average norm for the group (Appendix 2). B4 was probably derived from a predominantly felsic source of grantoid composition whilst B3 and B5 are less mature sediments from a source similar

to that of B4 with varying amounts of basic source rock contribution.

3.4 Ore Metals

The concentrations of Zn, Pb and Cu in the Slocan Group sediments are of interest as they are a possible source of the metals in the local ore deposits. Cu (Cu^{2+} ionic radius 0.72\AA) and Zn (ionic radius 0.74\AA) average concentrations for the five groups show a strong positive correlation with a correlation coefficient of 0.88 (Figure 18) and very similar geochemical patterns when plotted against Fe_2O_3 (Figures 19 and 20).

This indicates that Cu and Zn are probably present in the same iron silicate and oxide minerals in the sediment rather than occurring as disseminated sulphides. If Cu and Zn were in the sulphides, they would be unlikely to show such a strong correlation as they do not enter the same sulphide phase. Cu concentrations lie within the average range for argillaceous sediments whilst Zn concentrations are within and slightly above average values. Groups B2, B3 and B4 show little internal variation of Zn and Cu concentrations. B2 has values typical of basic rocks; the high SiO_2 members of B4 have low $\text{Fe}_2\text{O}_3\%$ and low Cu and Zn concentrations but the overall average for the group is typical of granodiorite and granitic rocks. Groups B5 and B1 have the highest average Cu and Zn concentrations. Within B5 there is a strong positive correlation between Fe_2O_3 and Cu and Zn and the high ore metal concentrations probably reflect high detrital Cu and Zn values in the iron silicates and oxides of the sediment. B1 has the largest internal variation and the highest concentrations of Cu and Zn in the five sedimentary groups. Cu and Zn concentrations show no correlation with Fe_2O_3 but are generally higher in the

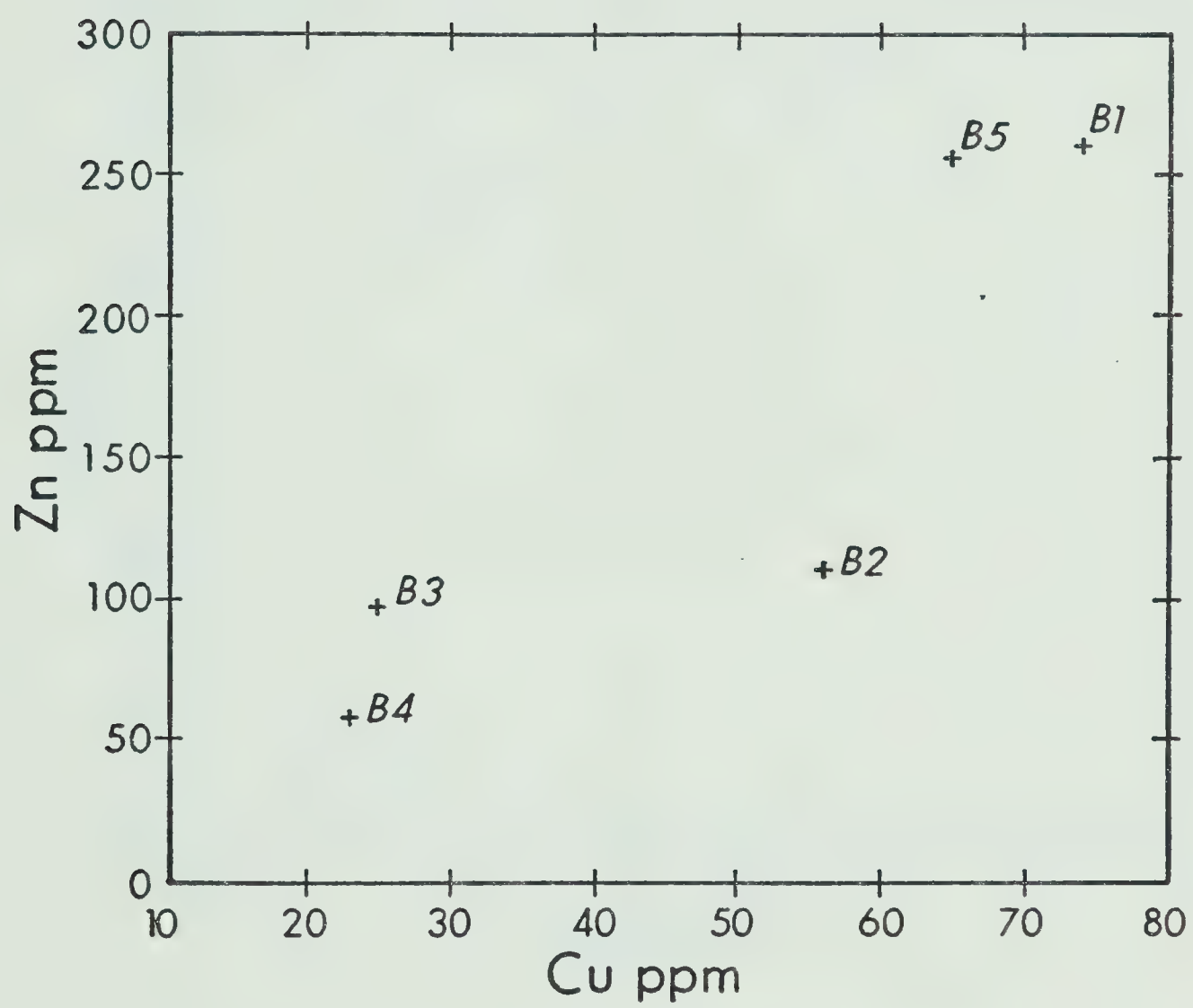


Figure 18. Zn versus Cu diagram.

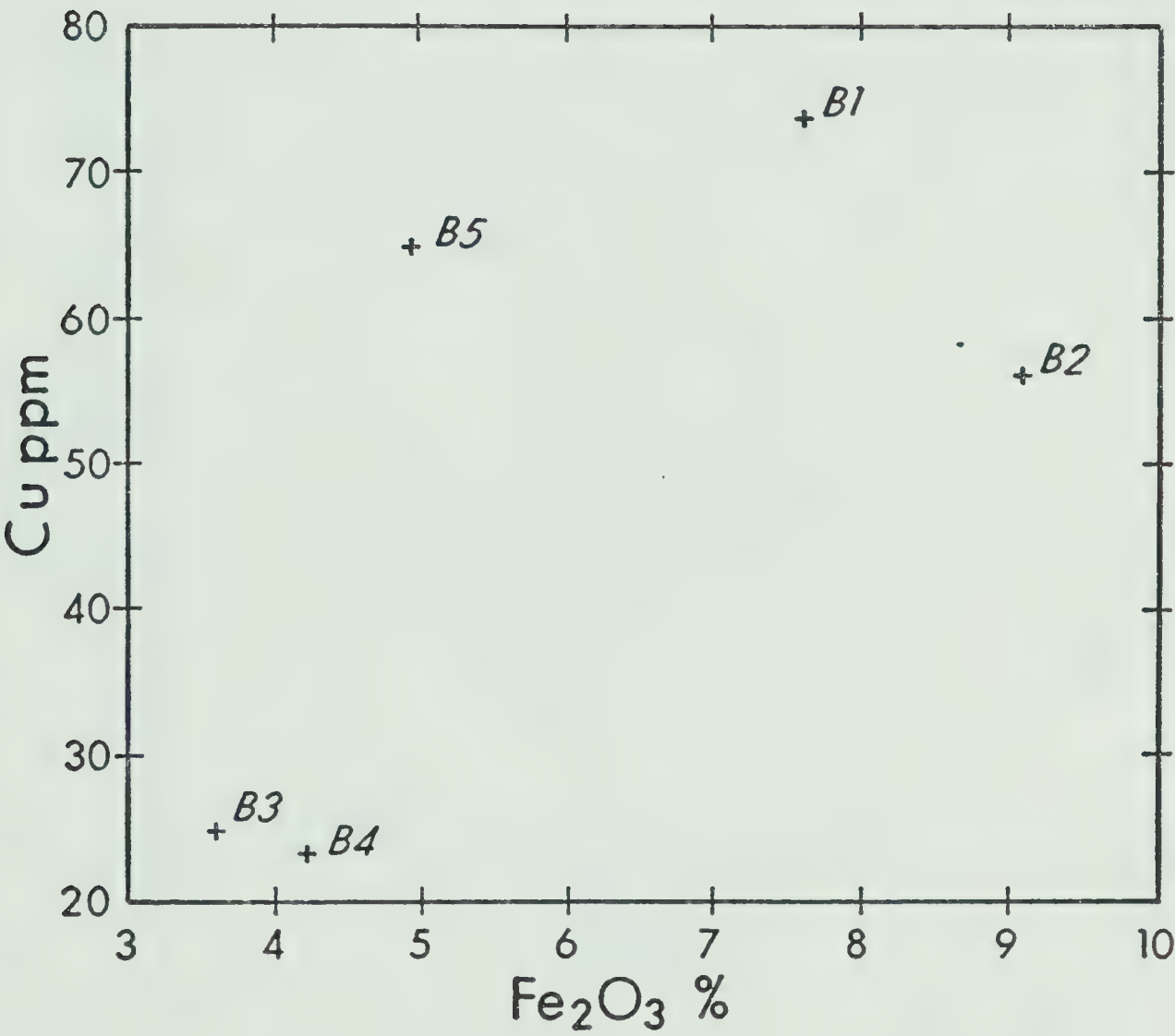


Figure 19. Fe₂O₃ (total) versus Cu diagram.

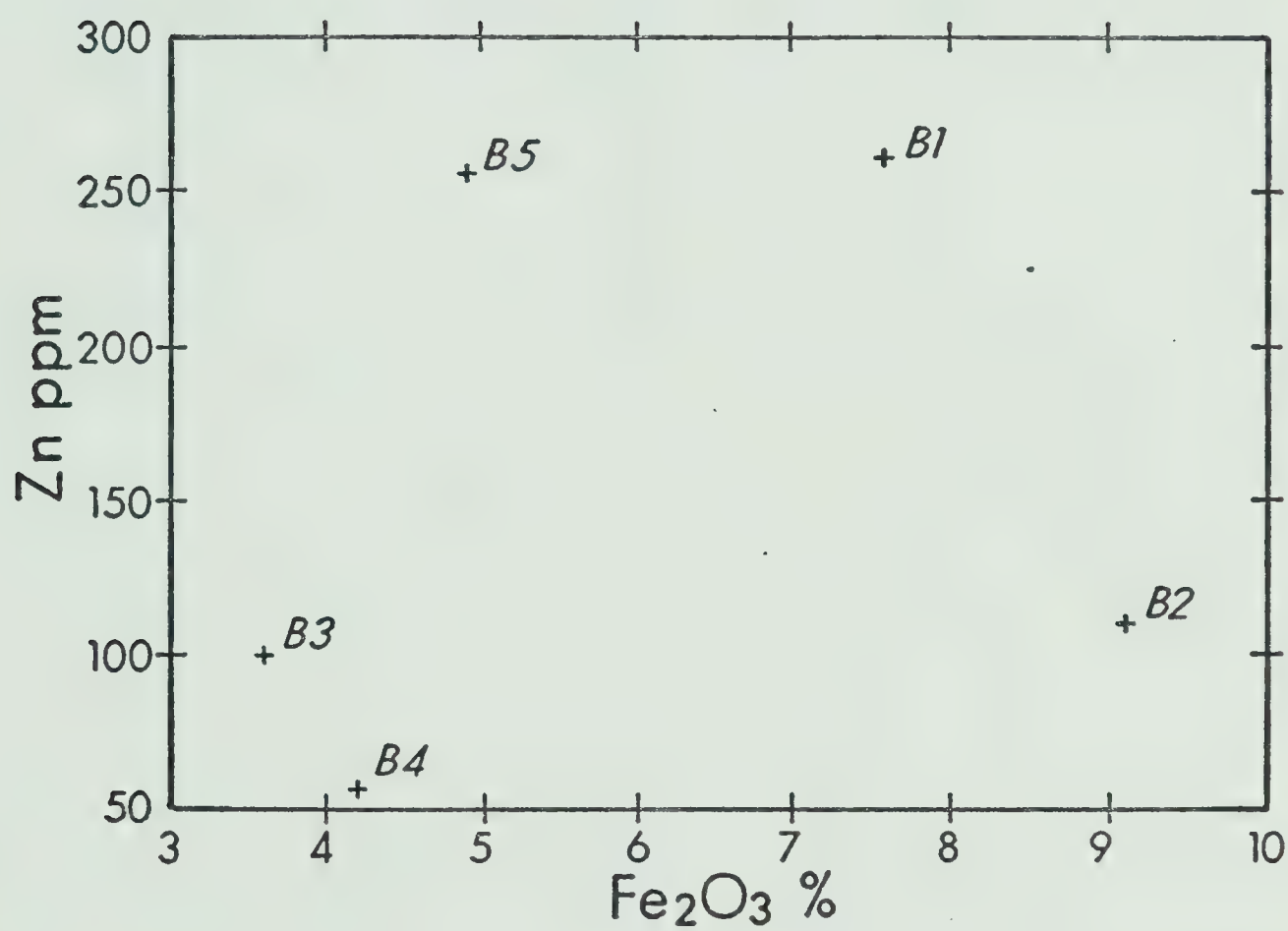


Figure 20. Fe₂O₃ (total) versus Zn diagram.

samples having high S values and the variation may be due to minor amounts of the sulphides in the sediment.

Pb (Pb^{2+} ionic radius 1.20\AA) concentrations in the sediments are at average crustal levels and show very little variation between different samples. Pb does not correlate with any other element, for example K (ionic radius 1.33\AA) (Figure 21) which it often follows geochemically, suggesting that the Pb has been remobilised and redistributed in the Slocan Group sediments and is probably present in a disseminated sulphide phase, a behaviour which is completely different from that of Cu and Zn.

In conclusion, the geochemistry of Cu, Zn and Pb in the Slocan Group sediments does not give any indication that the sediments are the source of the ore metals in the region. Pb and Zn concentration in ore depositing solutions is thought to originate either from partitioning between consolidating granitoid melts and their aqueous vapour phase or from leaching of country rock by hydrothermal solutions. While the geochemical evidence points to the unlikelihood of the latter process the argument is not foolproof. However, the isotopic composition of Pb is more definitive than simple Pb concentration for detecting genetic relationships between potential source rock and galena deposits and a lead isotope study of the region is the topic of the following section.

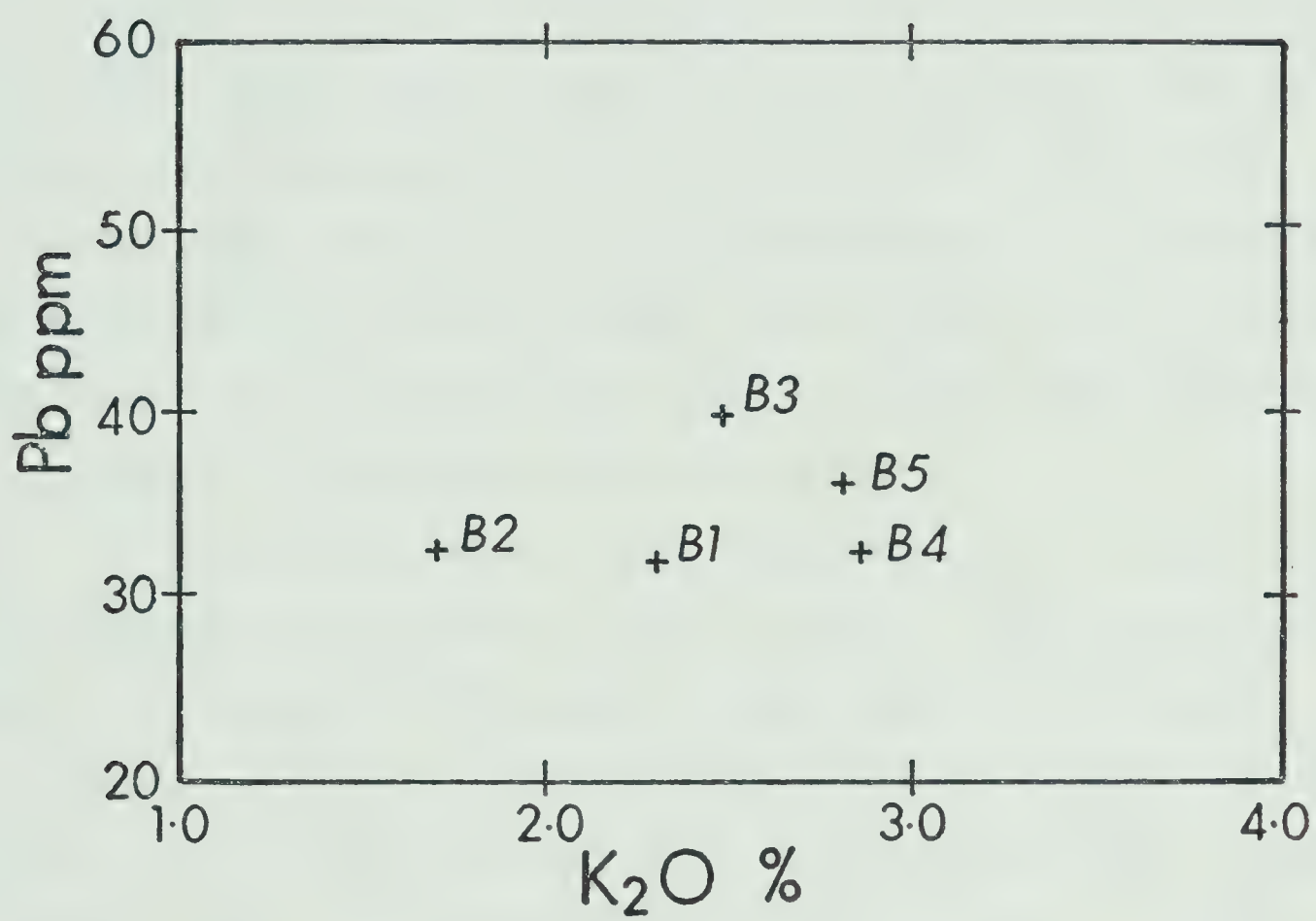


Figure 21. K_2O versus Pb diagram.

CHAPTER 4

LEAD ISOTOPES

The Pb-Zn-Ag mineral deposits of the region are found in both the Slocan Group sediments and the Nelson batholith. They are most abundant in the former where they are predominantly fissure deposits showing variable amounts of wall rock alteration. Their geology has been described in detail by various authors including Cairnes (1934), Hedley (1952), and Little (1960) and a genetic relationship between the ore deposits and the Nelson batholith has been implied. However Fyles (1967) has questioned this genetic link. Therefore lead isotope studies have been carried out to try and help clarify the problem of ore genesis.

The lead isotopic composition of seven galena and two pyrite samples were measured and the results are shown in Table 2. The maximum standard error, a combination of ^{204}Pb measuring error and fractionation error, is 0.1% per mass unit and is corrected for by normalising the ratios to the NBS 981 Pb isotope standard. Precision (2 σ) of the results is shown in the table and sample locations are displayed in Figure 4. The data is plotted on a conventional $^{207}\text{Pb}/^{204}\text{Pb}$ vs. $^{206}\text{Pb}/^{204}\text{Pb}$ diagram (Figure 22). Also shown on the diagram are the primary ore-lead growth curve from Stacey and Kramers (1975), previous data published by Reynolds and Sinclair (1971) on galenas from the area and K-feldspars from the Nelson batholith, lead isotope fields defined by Zartman (1974) and lead isotope composition ranges from Iceland and the Canaries (Sun and Jahn 1975). The lead isotope abundances generally coincide with those determined by

TABLE 2

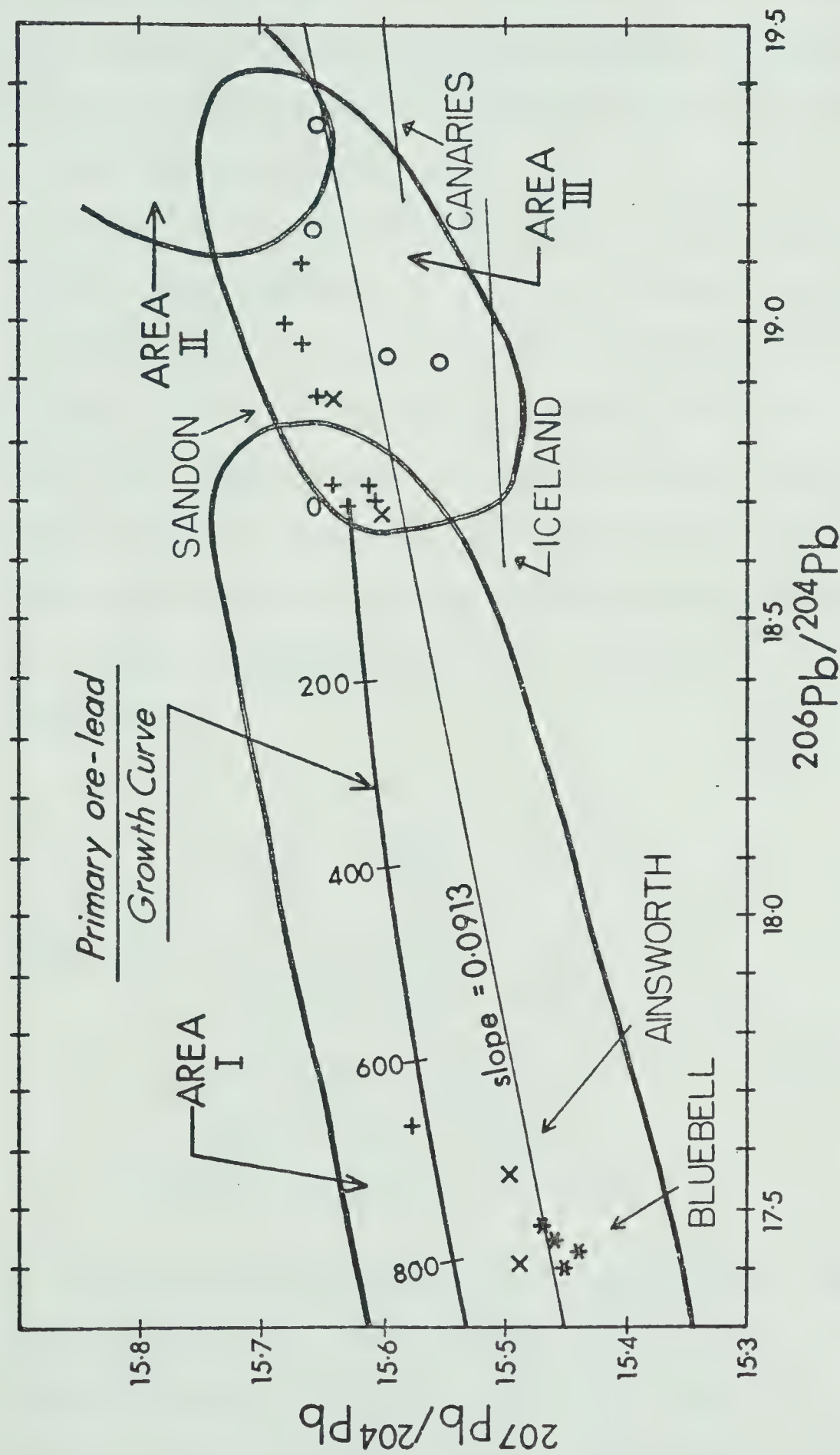
Isotopic composition of lead from galena and pyrite samples from near
or within the Nelson batholith

(errors shown are $\pm 2\sigma$ measurement precision)

(All ratios normalised to the NBS 981 Pb isotope standard)

(pyrite samples have -py suffix)

	$^{206}\text{Pb}/^{204}\text{Pb}$	$^{207}\text{Pb}/^{204}\text{Pb}$	$^{208}\text{Pb}/^{204}\text{Pb}$
SCR	18.996 ± 0.012	15.685 ± 0.016	38.899 ± 0.044
22W	18.724 ± 0.008	15.614 ± 0.008	39.020 ± 0.018
KB py	19.097 ± 0.020	15.672 ± 0.024	39.505 ± 0.058
4.13 py	18.875 ± 0.040	15.658 ± 0.032	39.103 ± 0.100
FL	18.724 ± 0.006	15.642 ± 0.012	38.985 ± 0.028
6.1	18.691 ± 0.010	15.631 ± 0.014	39.127 ± 0.028
X14	18.701 ± 0.008	15.608 ± 0.008	39.030 ± 0.008
KB	18.963 ± 0.010	15.669 ± 0.008	38.824 ± 0.036
OL	17.643 ± 0.008	15.579 ± 0.008	38.500 ± 0.020



Reynolds and Sinclair except that one sample from the Ainsworth camp (OL) has a distinctly higher $^{207}\text{Pb}/^{206}\text{Pb}$ ratio. Almost all the Sandon and Nelson batholith samples plot to the right of the primary ore-lead growth curve whilst the Ainsworth and Bluebell leads have considerably less radiogenic isotope ratios.

When only a small number of results are available the usual approach in lead isotope studies is to utilise a previously described model which is capable of explaining the observed isotope abundances. Where the data defines a linear relationship, the gradient of the line represents the $^{207}\text{Pb}/^{206}\text{Pb}$ ratio generated by radioactive decay in the source rock from which the leads derived their last radiogenic component. This two stage model for the origin of the lead was described by Russell and Farquhar (1960), and is the one applied by Reynolds and Sinclair. The gradient R is given by the formula:

$$R = \frac{1}{137.8} \frac{(e^{\lambda_1 t_1} - e^{\lambda_1 t_2})}{(e^{\lambda t_1} - e^{\lambda t_2})}$$

Where λ_1 is the ^{235}U decay constant,

λ is the ^{238}U decay constant,

t_1 is the time when the source rocks became a closed system with respect to U, Th and Pb,

t_2 is the time of mineralisation.

The time of mineralisation was shown by Hedley (1952) to be shortly after the emplacement of the batholith and was assumed to be 150 Ma, from which Reynolds and Sinclair obtained a value for t_1 of 1530 ± 100 Ma, but more recently determined uranium decay constants change this age to 1450 ± 100 Ma. Hence it was reasoned that the radiogenic component of

the ore and rock leads was generated in source rocks between 1450 Ma and 150 Ma ago. The Nelson rock leads and the ore leads in spatially related ore deposits were inferred to be genetically related. A deep crustal lead source, with variable contamination of magma and ore solutions by radiogenic lead during upward movement through upper crustal rocks, according to Reynolds and Sinclair, explained the observed lead isotope abundances.

Although the new data presented approximately coincide with Reynolds and Sinclair's the applicability of their model is questioned and an alternative model suggested. Bluebell and Ainsworth lead isotopic ratios are considerably less radiogenic than those from the Sardon camp and Nelson batholith, which is not to be expected if in fact the leads are related genetically. Also the gradient of the radiogenic lead line and its validity must be questioned because of the high $^{207}\text{Pb}/^{204}\text{Pb}$ ratio for the one Ainsworth camp sample measured.

Over the last fifteen years the isotope division of the U.S. Geological Survey has been determining the lead isotopic composition of a large number of plutonic and volcanic rocks and ore deposits from the Cordillera of the western United States. Three discrete provinces have been defined by Zartman (1974), by characteristic patterns in the lead isotopic compositions of these Mesozoic and Cenozoic rocks and hydrothermal ores. The isotopic composition within each province reflects the geology of the source region from which the lead was derived.

As well as the various lead isotope patterns dependent on the source of the lead there are variations in isotopic composition dependent on the age of the igneous rock or ore deposit. However these effects are normally only apparent when age differences of at least several hundred

million years are compared. With age differences of less than 200 Ma regional isotopic characteristics seem to dominate, therefore Mesozoic and Cenozoic results are used without time resolution.

The aforementioned provinces are shown on Figure 22 as Area I, Area II and Area III. In Area I there is a tendency for the lead to be depleted in its radiogenic component relative to the hypothetical primary ore-lead growth curve. This requires a source region in which the U/Pb ratio was lowered during part of the lead isotope development. The low U/Pb ratios of certain deeply eroded cratonic areas and the common close association of Area I type lead with outcropping basement rock implies that Area I contains lead derived principally from the Precambrian basement. Wide ranges in isotopic composition of ore leads result from the addition of upper crustal radiogenic lead as hydrothermal solutions migrate upwards through the crust.

Area III is typified by large plutonic masses, volcanics and thick eugeosynclinal sequences of Mesozoic and Cenozoic rocks, many resembling typical island arc assemblages rich in volcanic detritus. Igneous rock and ore leads have only a small range in isotopic composition in a field that essentially coincides with that of oceanic basalts. Whilst oceanic basalts reveal slightly lower $^{207}\text{Pb}/^{204}\text{Pb}$ ratios for given $^{206}\text{Pb}/^{204}\text{Pb}$ than Area III leads, pelagic sediments and basalts presumably altered by sea water interaction appear to be similar in lead isotope composition to the Area III leads (Armstrong and Cooper 1971). The preponderance of plutonic and volcanic rocks and associated sediments of eugeosynclinal origin implies a lead source material related to new continental growth. Subducted pelagic sediment and/or basaltic oceanic crust could supply the

lead by a process where the subducted rocks melt and return as igneous rocks in the island arc environment. Area II contains lead derived from sediments eroded from adjacent Precambrian rocks but as none of the samples measured fell in this region it will not be further considered.

From the descriptions of Area I and Area III it seems that lead isotopes may provide a convenient method of indicating the possible extent of the Precambrian basement, where it is not exposed at the surface, as well as giving important information on ore genesis.

The rock leads and ore leads associated with the Nelson batholith clearly fall into two groups. Sandon ore and Nelson batholith leads all plot within Area III. In addition the lead is in association with plutonic rocks (the Nelson batholith), volcanic rocks (the Rossland Group volcanics, to the south) and eugeosynclinal sediments (the Slocan Group) which are all characteristic of Area III. The lead in these rocks and ores is thus presumably derived from a source associated with new continental growth, possibly subducted sediment and/or basaltic oceanic crust. Alternatively, the lead may be of mantle derivation and be contaminated with varying small amounts of upper crustal radiogenic lead. Bluebell and Ainsworth ore leads, which have a different origin, fall in Area I; that is, lead derived from the Precambrian basement with a low U/Pb ratio.

The genetic link between the Sandon ores and the Nelson batholith seems to be clear, the lead in both being of oceanic association. In order to explain the occurrence of Area I lead, the hydrothermal system associated with the Nelson batholith must have passed through the Precambrian basement below the eastern part of the region and remobilised the Area I lead of the Bluebell and Ainsworth ores.

The position of the edge of the craton in the Western Cordillera is a much debated topic. The occurrence of Area I leads in the east of the region and Area III leads further west implies that the western edge of the craton is in the vicinity of Kootenay Lake. This agrees with the conclusion of Price (1979) drawn from his deep structural work on the southeastern Canadian Cordillera.

CHAPTER 5

CONCLUSIONS AND DISCUSSION

The most significant conclusions arrived at in the previous chapters are summarised below:

1. The Nelson batholith differentiated from a calc-alkaline magma which originated in the mantle wedge above a subduction zone.
2. The Slocan Group sediments have a distinct two-fold division with regard to their source. The highest beds in the sequence were derived from a basic source region whilst the lower members had a more highly siliceous source. Ore metals in the sediments have unexceptional concentrations although Pb behaves differently from Cu and Zn, probably occurring as a disseminated sulphide phase whilst Cu and Zn enter ferromagnesium silicate minerals.
3. The ore-lead is shown to be of dual origin by isotope abundances. In all but the easternmost deposits in the region the lead is of 'young' oceanic affinity characterised by the narrow range of $^{207}\text{Pb}/^{204}\text{Pb}$ and $^{206}\text{Pb}/^{204}\text{Pb}$ ratios just to the right of the primary ore-lead growth curve. The deposits of the Bluebell and Ainsworth camps contain much less radiogenic lead with lead derived at least in part from the Precambrian basement.

The above features of the geology of the region will be fitted into an island arc model for the evolution of the region during Late Triassic to Middle Jurassic times.

The tectonic evolution of the Canadian Cordillera of southern British Columbia has been described in terms of plate tectonic concepts by Monger et al (1972) and Griffiths (1977). By the late Permian a large wedge of

clastic sediments flanked the western edge of the North American craton and an ocean basin of unknown width lay to the west of the continent. Subduction of oceanic crust had apparently not yet begun. Extensive vulcanism commenced in the Middle Triassic along two linear belts, the Nicola-Takla volcanics of the Intermontane Belt and the Karmutsen volcanics of the Insular Belt. Monger et al (1972) suggested that the latter were oceanic tholeiites and that the former were erupted above an easterly dipping subduction zone whilst Griffiths (1977) proposed an alternative 'double subduction zone' model for the generation of the two volcanic groups. In Upper Triassic times the focus of magmatism shifted eastwards from the Nicola region, possibly due to the growth of the arc-trench gap with time (Dickinson 1974) and the calc-alkaline Rossland pyroclastic-rich volcanics were erupted in the Lower Jurassic. They typify the later stages of the Nicola-Takla arc and, relative to the Nicola Group, occur in a 'back arc' setting apparently related to the transition zone between a subsiding basin, the Rossland Trough, based on oceanic crust and a positive belt to the west.

From the Jurassic onwards the subduction zone shifted westwards in response, according to Monger et al (1972), to the early opening of the North Atlantic pushing the North American craton westwards and sealing off the old subduction zone. Griffiths (1977) proposes that the double subduction zone was only transitory and ceased when the intervening oceanic crust was consumed. The Middle Jurassic calc-alkaline magmas which formed the Nelson batholith were probably generated before the oceanward off-stepping of the subduction zone.

The local geology of the northwest margin of the Nelson batholith is fitted into the regional picture with the aid of three sketch cross sec-

tions of Upper Triassic, Lower Jurassic and Middle Jurassic times.

In the Upper Triassic (Figure 23) the Slocan Group sediments were probably derived from the felsic Castlegar gneisses to the west although it is possible that the source may have been to the north or east. Future studies on current directions could help solve this problem. Varying minor contributions from a more basic source rock, possibly the Kaslo Group volcanics, occurred as the sediments were deposited as distal turbidites in the Rossland Trough. By the Lower Jurassic (Figure 23), the evolution of the Rossland volcanics island arc provided a basic source rock for the uppermost beds in the Slocan Group. Overall compression between the oceanic and continental plates initiated folding in the Proterozoic and Palaeozoic sediments of the Kootenay Arc. Continued compression of the region during the Middle Jurassic resulted in the folding of the Slocan sediments. The Nelson batholith, generated above the subduction zone, was intruded at this time (Figure 23). The hydrothermal system associated with the batholith contained lead of oceanic affinity and, in the east of the region, remobilised lead from the Precambrian basement. It is probable that this lead was deposited in the ores of the Bluebell and Ainsworth camps.

The tectonic setting has been discussed in more detail by Beddoe-Stephens (1977) who defines the 'Rossland Break' fault zone as the boundary between the depositional trough and the positive area to the west. He proposes that the Rossland magmas were probably focussed along this line of weakness which was possibly a southern continuation of the Pinchi fault zone. The 'Rossland Break' may therefore also represent the site of subduction which caused the generation of the early Mesozoic Kaslo volcanics. If this is so then Archaean continental crust cannot extend west of the Rossland area which is in agreement with the conclusions drawn from the lead isotope work of this study.

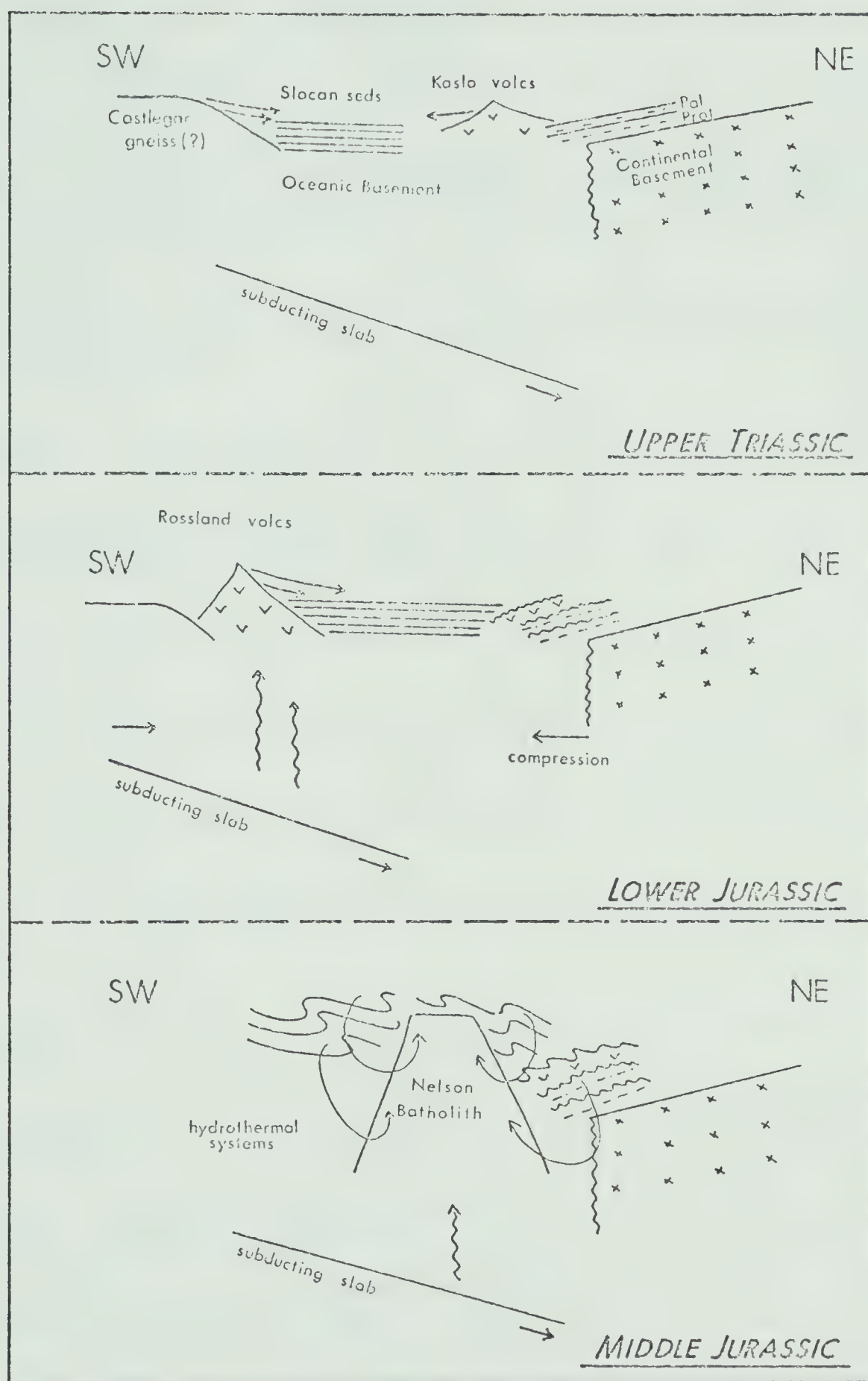


Figure 23. Sketch cross sections for the region during Upper Triassic, Lower Jurassic and Middle Jurassic times.

REFERENCES

- Armstrong, R.L. and Cooper, J.A. 1971. Lead isotopes in island arcs. *Bull. volcanol.*, vol. 35, pp. 27-63.
- Baadsgaard, H., Folinsbee, R.E. and Lipson, J., 1961. Potassium-argon dates of biotites from Cordilleran granites. *Bull. Geol. Soc. Amer.*, vol. 72, pp. 689-701.
- Beddoe-Stephens, B., 1977. The petrology and geochemistry of the Rossland volcanic rocks, southern British Columbia. Unpub. Ph.D. thesis, Durham University.
- Brame, S.L., 1979. Mineralisation near the northeast margin of the Nelson batholith. Unpub. M.Sc. thesis, University of Alberta.
- Buma, G., Frey, F.A. and Wanes, D.R., 1971. New England Granites: trace element evidence regarding their origin and differentiation. *Contrib. Mineral Petrol.*, vol. 31, pp. 300-320.
- Cairnes, C.E., 1934. Slocan Mining Camp, British Columbia. *Geol. Surv. Can. Mem.* 173.
- Cairnes, C.E., 1935. Descriptions of properties, Slocan Mining Camp, British Columbia. *Geol. Surv. Can., Mem.* 184.
- Carmichael, I.S.E., Turner, F.J. and Verhoogen, J., 1974. *Igneous Petrology*, McGraw-Hill, New York.
- Chappell, B.W., 1978. Granitoids from the Moonbi district, New England batholith, Eastern Australia. *J. Geol. Soc. Aust.*, vol. 25, pp. 267-283.
- Chappell, B.W. and White, A.J.R., 1974. Two contrasting granite types. *Pacific Geology*, vol. 8, pp. 173-174.
- Coleman, R.G., 1965. Composition of jadeitic pyroxene from the California metagreywackes. *U.S. Geol. Surv. Prof. Paper* 525-C, pp. 25-34.
- Condie, K.C., 1967. Geochemistry of early Precambrian greywackes from Wyoming. *Geochim. et Cosmochim. Acta*, vol. 31, pp. 2135-2149.
- Crosby, P., 1968. Tectonic, plutonic and metamorphic history of the central Kootenay Arc, British Columbia. *Geol. Soc. Am. Spec. Paper*, 99.
- Culbert, R.R., 1972. Abnormalities in the distribution of K, Rb and Sr in the Coast Mountains batholith, British Columbia. *Geochim. et Cosmochim. Acta*, vol. 36, pp. 1091-1100.
- Cumming, G.L. and Richards, J.R., 1975. Ore lead isotope ratios in a continuously changing earth. *Earth Planet Sci. Lett.*, vol. 28, pp. 155-171.

- Dickinson, W.R., 1974. Width of modern arc-trench gaps proportional to past duration of igneous activity in associated magmatic arcs. *J. Geophys. Res.*, vol. 78, pp. 3376-3389.
- Dickinson, W.R., 1976. Sedimentary basins developed during the evolution of Mesozoic-Cenozoic arc trench systems in western North America. *Can. J. Earth Sci.*, Vol. 13, pp. 1268-1287.
- Dodge, F.C.W., 1972. Trace element content of some plutonic rocks of the Sierra Nevada batholith. *U.S. Geol. Surv. Bull.*, 1314-F.
- Doe, B.R., and Stacey, J.S., 1974. The application of lead isotopes to the problem of ore genesis and ore prospect evaluation: a review. *Econ. Geol.*, vol. 69, pp. 757-776.
- Douglas, R.J.W., Gabrielse, H., Wheeler, J.O., Stott, D.F. and Belyea, H.R., 1970. Geology of Western Canada; Chap. 7 in *Geology and Economic Minerals of Canada*. *Geol. Surv. Can., Econ. Geol. Rept.* 1, pp. 367-488.
- Duncan, I.J., Parrish, R.R. and Armstrong, R.L., 1979. Rb/Sr geochronology of post-tectonic intrusive events in the Omineca Crystalline Belt, southeastern British Columbia. *Geological Association of Canada, Cordilleran Section, Programme and Abstracts*, p. 15.
- Fairbairn, H.W., Hurley, P.M. and Pinson W.H., 1964. Initial $^{87}\text{Sr}/^{86}\text{Sr}$ and possible sources of granitic rocks in southern British Columbia. *Jour. Geophys. Res.*, vol. 69, pp. 4889-4893.
- Faure, G., 1977. *Isotope Geology*. John Wiley and Sons, New York.
- Flanagan, F.J., 1973. 1972 values for international geochemical reference samples. *Geochim. et Cosmochim. Acta*, vol. 37, pp. 1189-1200.
- Fyles, J.T., 1966. Lead-zinc deposits in British Columbia. In: *Tectonic history and mineral deposits of the western Cordillera*. *Can. Inst. Mining Metal., Spec. vol.* No. 8, pp. 231-238.
- Fyles, J.T., 1967. Geology of the Ainsworth-Kalso area. *British Columbia Dept. Mines and Petrol. Res., Bull.* 53.
- Gabrielse, H. and Reesor, J.E., 1964. Geochronology of plutonic rocks in two areas of the Canadian Cordillera. *Roy. Soc. Can., Spec. Pub.*, vol. 8, *Geochronology in Canada*, pp. 96-138.
- Gabrielse, H. and Reesor, J.E., 1974. The nature and setting of granite plutons in the central and eastern parts of the Canadian Cordillera. *Pacific Geology*, vol. 8, pp. 109-138.
- Goldberg, E.D. and Arrhenius, G.O.S., 1958. Chemistry of the Pacific Pelagic sediments. *Geochim. et Cosmochim. Acta*, vol. 13, pp. 153-212.

- Green, T.H., 1972. Crystallisation of calc-alkaline andesite under controlled high pressure conditions. *Contrib. Mineral. and Petrol.*, vol. 34, pp. 150-166.
- Green, T.H. and A.E. Ringwood, 1968. Genesis of the calc-alkaline igneous rock suite. *Contrib. Mineral. and Petrol.* vol. 18, pp. 105-162.
- Griffiths, J.R., 1977. Mesozoic-early Cenozoic volcanism, plutonism, and mineralisation in southern British Columbia: a plate tectonic synthesis. *Can. Jour. Earth Sci.*, vol. 14, pp. 1611-1624.
- Hall-Beyer, B.M., 1976. Geochemistry of some ocean-floor basalts of central British Columbia. Unpub. M.Sc. thesis, University of Alberta.
- Hansen, G.N., 1978. The application of trace elements to the petrogenesis of igneous rocks of granitic composition. *Earth Planet Sci. Letters*, vol. 38, pp. 26-43.
- Hedley, M.S., 1952. Geology and ore deposits of the Sardon area, Slocan mining camp, British Columbia. *British Columbia Dept. Mines and Petrol. Res.*, Bull. 29.
- Hine, R., Williams, I.S., Chappell, B.W. and White, A.J.R., 1978. Contrasts between I- and S-type granitoids of the Kosciusko batholith. *J. Geol. Soc. Aust.*, vol. 25, pp. 339-355.
- Hoy, T., 1976. Calc-silicate isograds in the Riondel area, southeastern British Columbia. *Can. J. Earth Sci.*, vol. 13, pp. 1093-1104.
- Hoy, T., 1977. Stratigraphy and structure of the Kootenay Arc in the Riondel area, southeastern British Columbia. *Can. J. Earth Sci.*, vol. 14, pp. 2301-2315.
- Irwin, A.B., 1951. Mapping complex folds in the Slocan Series, British Columbia. *Trans. Can. Inst. Mining Met.*, vol. 54, pp. 494-501.
- Irwin, A.B., 1952. Discussion on mapping complex folds in the Slocan Series, British Columbia. *Trans. Can. Inst. Mining Met.*, vol. 55, pp. 242-244.
- Kanasewich, E.R., 1968. The interpretation of lead isotopes and their geological significance. In: *Radiometric dating for geologists*, pp. 147-223, Interscience, New York.
- Kolbe, P. and Taylor, S.R., 1966. Geochemical investigation of the granitic rocks of the Snowy Mountains area, New South Wales. *J. Geol. Soc. Aust.*, vol. 13, pp. 1-25.
- Lambert, R. St J. and Holland, J.G., 1977. Trace elements and petrogenesis of DSDP 37 basalts. *Can. J. Earth Sci.*, vol. 14, pp. 809-836.
- Little, H.W., 1960. Nelson Map-area, west half, British Columbia. *Geol. Surv. Can.*, Mem. 308.

- Margaritz, M. and Taylor H.P., 1977. Water-rock interactions in the granitic batholiths of British Columbia, part III, pp. 80-89. Proceedings of the 2nd international symposium on water-rock interaction, Strasbourg, France.
- Monger, J.W.H., 1975. Correlation of eugeosynclinal tectono-stratigraphic belts in the North American Cordillera. Geoscience Canada, vol. 2, pp. 4-10.
- Monger, J.W.H., Souther, J.G., and Gabrielse, H., 1972. Evolution of the Canadian Cordillera: a plate tectonic model. Am. Jour. Sci., vol. 272, pp. 577-602.
- Nguyen, K.K., Sinclair, A.J. and Libby, W.G., 1968. Age of the northern part of the Nelson batholith. Can. J. Earth Sci., vol. 5, pp. 955-957.
- Nockolds, S.R., 1954. Average chemical compositions of some igneous rocks. Geol. Soc. Amer. Bull., vol. 65, pp. 1007-1032.
- Pettijohn, F.J., 1957. Sedimentary Rocks (2nd edition), Harper.
- Price, R., 1979. The margin of the North American craton in the southeastern Canadian Cordillera. Geological Association of Canada, Cordilleran Section, Programme and Abstracts, p. 25.
- Reynolds, P.H. and Sinclair, A.J., 1971. Rock and ore-lead isotopes from the Nelson batholith and the Kootenay Arc, British Columbia. Econ. Geol., vol. 66, pp. 259-266.
- Rice, H.M.A., 1941. Nelson map area, east half, British Columbia. Geol. Surv. Can., Mem. 228.
- Ringwood, A.E., 1974. The petrological evolution of island arc systems. Jl. geol. Soc. Lond., vol. 130, pp. 183-204.
- Ross, J.V., 1970. Structural evolution of the Kootenay Arc, southeastern British Columbia. Geol. Assoc. Can., Spec. Paper 6, pp. 53-65.
- Ross, J.V. and Kellerhals, P., 1968. Evolution of the Slocan Syncline in south-central British Columbia. Can. J. Earth Sci., vol. 5, pp. 851-872.
- Russell, R.D. and Farquhar, R.M., 1960. Lead isotopes in geology. Interscience, New York.
- Stacey, J.S. and Kramers, J.D., 1975. Approximation of terrestrial lead isotope evolution by a two stage model. Earth Planet. Sci. Lett., vol. 26, pp. 207-221.
- Sun, S.S. and Jahn, B.M., 1975. Lead and strontium isotopes in post-glacial basalts from Iceland. Nature, vol. 255, pp. 527-530.

- Tauson, L.V., 1967. Geochemical behaviour of rare elements during crystallisation and differentiation of granitic magmas. *Geochem. Int.*, vol. 4, pp. 1067-1075.
- Taylor, S.R., 1965. The application of trace element data to problems in petrology. *Phys. Chem. of the Earth*, vol. 6, pp. 133-213.
- Taylor, S.R., Capp, A.C., Graham, A.L. and Blake, D.H., 1969. Trace element abundances in andesites. *Contrib. Mineral. and Petrol.*, vol. 23, pp. 1-26.
- Wedepohl, K.H., (Exec. Ed.), 1969. *Handbook of Geochemistry*, Springer-Verlag, New York.
- Wheeler, J.O. and Gabrielse, H., 1972. The Cordilleran Structural province; in *Variations in Tectonic styles*, *Geol. Assoc. Can. Spec. Paper*, vol. 11, pp. 2-81.
- White, A.J.R. and Chappell, B.W., 1977. Ultrametamorphism and granitoid genesis. *Tectonophysics*, vol. 43, pp. 7-22.
- Winzer, S.R., 1973. Metamorphism and chemical equilibrium in some rocks from the central Kootenay Arc. Unpub. Ph.D. thesis, University of Alberta.
- Wyllie, P.J., Huang, W-L., Stern, C.R. and Malloee S., 1976. Granitic magmas: possible and impossible sources, water contents and crystallisation sequences. *Can. J. Earth Sci.*, vol. 13, pp. 1007-1019.
- Zartman, R.E., 1974. Lead isotope provinces in the Cordillera of the western United States and their geological significance. *Econ. Geol.*, vol. 69, pp. 792-805.
- Zartman, R.E. and Stacey, J.S., 1971. Lead isotopes and mineralisation ages in Belt Supergroup rocks, northwestern Montana and northern Idaho. *Econ. Geol.*, vol. 66, pp. 849-860.

APPENDIX 1

Chemical analyses, approximate modal analyses and norms of the Nelson
batholith samples

Samples 7.1, 7.2, 7.3, 7.6, 7.7, 7.10, 7.12, 7.13 are from the main body
of the batholith.

Samples 7.8, 7.9, 7.14, 7.15 are from the border rocks.

Samples 7.17, 7.18, 7.19, 7.20, 7.21, 7.22, 7.23, 7.24 are from porphyry
bodies.

Sample 7.16 is the hololeucocratic granite.

Samples 7.4, 7.5 are from the xenolith.

a) Chemical analyses (major elements as weight % of oxides, trace elements in ppm).

Sample Number	7.1	7.2	7.3	7.4	7.5	7.6	7.7
SiO ₂	67.00	66.61	66.81	56.02	54.64	65.29	63.24
Al ₂ O ₃	15.52	16.55	15.58	13.47	13.27	16.23	16.62
Total Fe as Fe ₂ O ₃	4.12	3.57	4.00	7.68	7.99	4.50	5.09
MgO	1.21	1.19	0.99	10.25	10.22	1.78	1.89
CaO	3.27	4.44	4.17	4.79	6.33	4.73	5.47
Na ₂ O	3.63	4.35	4.26	2.40	2.54	3.48	3.67
K ₂ O	4.46	2.61	3.34	3.99	3.50	2.95	2.95
TiO ₂	0.50	0.41	0.51	0.88	0.96	0.55	0.61
MnO	0.09	0.07	0.10	0.12	0.13	0.12	0.13
P ₂ O ₅	0.19	0.19	0.23	0.39	0.40	0.36	0.32
S	0.01	0.01	0.01	0.02	0.02	0.02	0.01
Pb	40	33	37	33	33	37	37
Ba	1191	1063	911	1540	1164	1554	1220
Nb	28	20	36	23	18	25	33
Zr	128	127	195	148	147	130	150
Y	20	13	21	19	19	16	19
Sr	658	736	1050	594	736	766	788
Rb	154	85	93	128	79	75	76
Zn	83	58	96	113	100	83	88
Cu	9	4	18	10	27	9	7
Ni	5	5	5	230	238	4	6
Cr	12	7	12	458	431	8	7
V	63	50	70	110	113	75	88
V/Ni	12.6	10.0	14.0	0.5	0.5	18.8	12.6
K/Rb	240	255	299	258	368	326	322

Sample Number	7.8	7.9	7.10	7.11	7.12	7.13	7.14
SiO ₃	53.81	52.00	62.80	65.76	65.24	65.09	62.91
Al ₂ O ₃	15.49	13.30	15.81	15.58	16.17	16.14	14.64
Total Fe as Fe ₂ O ₃	10.22	11.67	6.08	4.42	4.65	4.25	5.83
MgO	5.21	6.51	1.88	1.00	1.19	1.06	2.59
CaO	6.46	9.62	4.04	4.06	3.57	3.38	5.43
Na ₂ O	3.82	2.36	4.10	3.88	4.26	3.94	3.69
K ₂ O	2.99	2.06	3.95	4.44	3.94	5.27	3.61
TiO ₂	1.13	1.37	0.87	0.54	0.57	0.53	0.69
MnO	0.17	0.23	0.14	0.10	0.10	0.12	0.11
P ₂ O ₅	0.68	0.82	0.26	0.18	0.25	0.17	0.44
S	0.02	0.07	0.07	0.03	0.06	0.04	0.03
Pb	30	36	33	42	37	43	37
Ba	1161	1152	1039	1273	1343	1799	1231
Nb	17	18	46	41	40	47	16
Zr	132	78	251	234	237	228	121
Y	19	30	29	27	26	26	17
Sr	1382	1065	1082	1077	1186	915	1062
Rb	74	41	135	133	104	150	79
Zn	126	136	127	92	107	115	89
Cu	54	46	17	9	20	16	30
Ni	18	18	2	6	7	2	13
Cr	53	55	18	10	14	9	35
V	219	294	63	63	63	50	150
V/Ni	12.2	16.3	31.5	10.5	9	25	11.5
K/Rb	335	417	242	277	314	291	378

Sample Number	7.15	7.16	7.17	7.18	7.19	7.20	7.21
SiO ₂	60.75	71.99	60.86	59.57	65.93	65.21	65.60
Al ₂ O ₃	14.54	15.59	14.80	15.14	15.19	15.20	15.46
Total Fe as Fe ₂ O ₃	7.03	1.12	6.09	7.80	4.37	4.84	4.58
MgO	3.14	0.31	2.49	3.40	1.53	2.01	1.65
CaO	6.24	0.97	6.52	6.65	4.81	5.02	4.17
Na ₂ O	3.63	5.43	4.53	3.12	4.19	4.03	3.92
K ₂ O	3.17	4.38	3.61	3.08	3.09	2.85	3.29
TiO ₂	0.82	0.12	0.54	0.59	0.42	0.42	0.42
MnO	0.13	0.03	0.15	0.17	0.12	0.11	0.36
P ₂ O ₅	0.55	0.04	0.31	0.42	0.25	0.26	0.20
S	0.01	0.01	0.10	0.05	0.10	0.05	0.35
Pb	33	40	33	33	37	37	18
Ba	1223	1493	1354	1343	1557	1533	1704
Nb	16	13	11	10	15	13	11
Zr	136	120	102	69	107	86	119
Y	17	6	14	14	13	11	12
Sr	1167	1371	972	672	886	888	1140
Rb	57	87	83	60	55	56	68
Zn	95	111	79	98	156	82	--
Cu	17	12	32	11	32	9	--
Ni	14	2	5	4	4	3	--
Cr	43	4	26	18	16	19	--
V	163	19	125	163	88	113	--
V/Ni	11.6	9.5	25	40.8	22.0	37.7	--
K/Rb	461	417	316	426	466	422	402

Sample Number	7.22	7.23	7.24
SiO ₂	63.10	64.64	63.05
Al ₂ O ₃	15.46	15.00	15.13
Total Fe as Fe ₂ O ₃	5.95	5.66	6.28
MgO	2.58	2.54	2.91
CaO	5.19	4.65	5.11
Na ₂ O	3.61	3.52	3.16
K ₂ O	2.86	2.96	3.15
TiO ₂	0.47	0.47	0.53
MnO	0.36	0.08	0.08
P ₂ O ₅	0.31	0.31	0.34
S	0.11	0.16	0.25
Pb	13	11	39
Ba	1477	1639	1596
Nb	10	8	8
Zr	89	96	91
Y	12	12	13
Sr	883	822	822
Rb	58	54	61
K/Rb	409	455	429

b) Approximate modal analyses

	7.1	7.2	7.3	7.4	7.5	7.6	7.7	7.8	7.9
Quartz	20	20	20	<5	<5	15	10	<5	<5
Plagioclase Feldspar	50	45	55	30	35	60	60	35	40
K feldspar	20	20	10	20	15	20	20	25	15
Hornblende	minor	5	15	30	40		minor	35	40
Biotite	5	10	minor	20	10		10	<5	<5
Chlorite	5					5			
Epidote	minor	minor				minor	minor		

& accessory sphene and opaque oxides

	7.10	7.11	7.12	7.13	7.14	7.15	7.16	7.17	7.18
Quartz	10	20	25	20	10	<5	30	10	15
Plagioclase Feldspar	60	50	45	45	45	45	30	55	55
K Feldspar	20	15	20	25	25	25	40	15	10
Hornblende		10			10	25		minor	
Biotite								20	20
Chlorite	10	5	10	10	10	5	minor		
Epidote	minor		minor	minor	minor		minor	minor	minor

& accessory sphene and opaque oxides

	7.19	7.20	7.21	7.22	7.23	7.24
Quartz	30	30	25	15	20	20
Plagioclase Feldspar	50	50	55	50	50	50
K Feldspar	10	10	10	15	15	15
Hornblende				15	10	15
Biotite			10	5	5	minor
Chlorite	10	10	minor			
Epidote	minor	minor		minor	minor	minor

& accessory sphene and opaque oxides

c) Norms	7.1	7.2	7.3	7.4	7.5	7.6	7.7	7.8	7.9	7.10	7.11	7.12
Qz	19.0	19.5	18.7	--	--	19.9	15.4	--	1.0	11.4	15.9	14.9
Or	26.5	15.5	19.8	23.7	20.8	17.5	17.5	17.8	12.3	23.5	26.3	23.4
Ab	30.8	36.9	36.1	20.8	21.6	29.6	31.2	32.6	20.2	34.8	32.9	36.2
An	12.9	17.9	13.5	14.2	14.5	20.0	20.2	16.4	19.8	13.1	12.0	13.4
Di	2.8	3.5	6.1	7.7	13.7	3.0	5.9	13.1	23.3	5.9	7.0	3.7
Hyp	5.7	4.6	3.3	29.0	18.9	7.4	6.9	6.9	16.6	7.5	3.3	5.7
Ol	--	--	--	0.5	5.8	--	--	7.3	--	--	--	--
Mt	1.5	1.3	1.5	2.8	2.9	1.6	1.8	3.7	4.3	2.2	1.6	1.7
Ilm	1.0	0.8	1.0	1.7	1.8	1.1	1.2	2.2	2.6	1.7	1.0	1.1
Cor	--	--	--	--	--	--	--	--	--	--	--	--

	7.13	7.14	7.15	7.16	7.17	7.18	7.19	7.20	7.21	7.22	7.23	7.24
Qz	12.7	12.7	10.1	20.5	5.2	9.9	17.5	17.1	18.1	15.3	18.0	16.1
Or	31.3	21.5	18.9	25.9	21.5	18.3	18.4	16.9	19.6	17.0	17.6	18.8
Ab	33.4	31.4	30.9	45.8	38.5	26.5	35.6	34.2	33.4	30.8	29.9	26.9
An	10.8	12.8	14.1	5.2	9.4	18.3	13.5	15.0	15.0	17.6	16.4	17.9
Di	5.1	11.8	14.1	--	19.1	12.3	8.7	8.3	4.9	6.9	5.6	6.3
Hyp	4.2	6.4	7.9	1.9	3.1	10.7	3.9	5.9	6.4	9.3	9.5	10.8
Ol	--	--	--	--	--	--	--	--	--	--	--	--
Mt	1.5	2.1	2.6	0.4	2.2	2.8	1.6	1.8	1.6	2.2	2.1	2.2
Ilm	1.0	1.3	1.6	0.2	1.0	1.1	0.8	0.8	0.8	0.9	0.9	1.0
Cor	--	--	--	0.1	--	--	--	--	--	--	--	--

APPENDIX 2

Chemical analyses, mineral assemblages and norms for the Slocan Group
sediments

a) Chemical analyses

(major elements as weight % oxides, trace elements in ppm. ND = not determined)

Bl	Sample No.	1.1	1.2	1.3	1.4	1.5	1.6	1.7
SiO ₂		74.50	73.88	60.42	54.78	62.52	68.63	60.25
Al ₂ O ₃		12.92	8.50	16.91	16.46	14.68	13.00	15.94
Total Fe as Fe ₂ O ₃		3.76	5.34	6.74	8.59	6.60	6.12	9.55
MgO		1.76	1.36	4.07	6.33	3.41	2.54	4.40
CaO		1.14	7.84	3.99	6.64	5.70	3.43	2.22
Na ₂ O		1.15	0.76	3.42	3.03	3.61	3.08	2.17
K ₂ O		3.32	0.64	2.59	2.52	1.66	1.68	2.75
TiO ₂		0.66	0.40	0.62	0.87	0.65	0.55	0.66
MnO		0.04	0.10	0.07	0.18	0.08	0.07	0.08
P ₂ O ₅		0.18	0.15	0.22	0.34	0.25	0.18	0.28
S		0.54	1.03	0.93	0.27	0.84	0.72	1.72
Pb		22	27	33	33	33	33	36
Ba		1865	293	1820	2515	1352	1339	1427
Nb		15	11	6	5	7	8	9
Zr		130	137	106	70	89	82	102
Y		36	36	22	21	25	20	33
Sr		165	291	391	613	508	362	191
Rb		92	23	64	76	37	45	91
Zn		523	791	127	232	188	228	236
Cu		73	106	67	52	89	67	198
Ni		45	28	2	21	34	23	33
Cr		165	43	37	130	90	85	142
V		475	175	200	181	275	288	475

	1.8	1.9	1.10	1.11	1.12	1.13	1.14
SiO ₂	58.98	50.19	45.87	54.08	54.48	62.87	54.05
Al ₂ O ₃	14.64	13.21	10.82	16.38	16.17	13.92	16.50
Total Fe as Fe ₂ O ₃	6.63	10.88	9.92	10.09	9.57	7.47	9.36
MgO	3.47	9.98	6.55	6.21	7.17	3.74	5.48
CaO	7.35	11.40	21.66	5.06	4.60	5.58	6.55
Na ₂ O	2.18	2.49	2.69	4.26	3.86	2.28	4.23
K ₂ O	4.05	0.34	0.44	2.10	2.67	2.74	2.12
TiO ₂	0.76	0.85	0.76	1.12	1.00	0.72	1.03
MnO	0.10	0.18	0.34	0.15	0.12	0.08	0.14
P ₂ O ₅	0.33	0.24	0.31	0.33	0.29	0.17	0.33
S	1.50	0.23	0.64	0.23	0.07	0.42	0.22
Pb	36	ND	ND	33	30	33	30
Ba	1203	522	1288	1918	1840	2560	2399
Nb	7	7	7	8	6	7	4
Zr	91	66	67	77	76	62	88
Y	29	17	17	20	20	16	19
Sr	267	526	639	565	564	509	694
Rb	95	4	7	38	47	45	48
Zn	133	133	112	122	114	469	111
Cu	91	57	111	72	28	96	46
Ni	95	201	56	14	32	46	26
Cr	74	704	193	174	137	133	110
V	375	ND	ND	263	200	350	200

	1.15	1.16	1.17	1.18	1.19	1.20
SiO ₂	58.31	52.45	59.09	54.62	61.79	57.63
Al ₂ O ₃	16.96	7.92	12.93	16.34	14.74	17.03
Total Fe as Fe ₂ O ₃	8.00	6.49	6.63	9.06	7.57	7.66
MgO	4.56	3.08	2.92	5.24	3.60	4.32
CaO	3.22	24.33	12.03	6.77	5.02	4.70
Na ₂ O	4.54	2.42	3.70	4.62	4.11	5.46
K ₂ O	2.81	1.55	1.15	1.80	1.63	1.85
TiO ₂	0.91	0.81	0.61	0.93	0.75	0.84
MnO	0.09	0.23	0.14	0.15	0.09	0.12
P ₂ O ₅	0.27	0.32	0.29	0.32	0.22	0.30
S	0.33	0.31	0.50	0.15	0.48	0.08

Pb	33	ND	ND	33	33	33
Ba	1191	513	659	933	561	1059
Nb	9	9	6	7	9	6
Zr	101	120	80	82	75	78
Y	22	24	25	20	20	20
Sr	450	415	476	540	608	677
Rb	86	35	29	58	45	36
Zn	248	348	354	104	410	103
Cu	64	45	63	35	66	34
Ni	28	20	25	17	50	17
Cr	82	47	63	76	171	78
V	300	ND	ND	194	319	163

<u>B2</u>	Sample No.	2.1	2.2	2.3	2.4	2.5	2.6	2.7
SiO ₂		54.92	60.81	57.00	50.18	49.35	49.32	65.05
Al ₂ O ₃		16.54	14.78	16.97	15.14	14.46	16.50	12.29
Total Fe as Fe ₂ O ₃		9.43	6.86	7.86	9.78	10.20	10.69	8.08
MgO		5.43	3.33	4.34	11.46	11.98	10.39	5.62
CaO		5.87	6.04	5.10	6.01	7.10	4.72	4.05
Na ₂ O		5.40	5.96	5.90	4.17	3.86	3.78	2.05
K ₂ O		0.81	0.75	1.35	1.89	1.76	3.11	1.68
TiO ₂		0.95	0.80	0.85	0.89	0.83	0.99	0.70
MnO		0.15	0.10	0.13	0.14	0.16	0.15	0.10
P ₂ O ₅		0.31	0.30	0.28	0.27	0.28	0.33	0.14
S		0.18	0.28	0.22	0.08	0.02	0.03	0.25
Pb		33	35	36	27	28	23	33
Ba		672	866	1284	584	352	1036	1469
Nb		6	9	8	5	2	4	5
Zr		72	109	86	53	44	50	56
Y		18	23	18	19	16	21	12
Sr		645	564	671	453	633	349	373
Rb		18	11	25	28	30	63	37
Zn		108	136	100	83	84	87	90
Cu		35	53	14	93	72	90	66
Ni		26	21	14	147	175	119	70
Cr		116	57	51	392	333	305	168
V		213	213	167	213	181	181	150

	2.8	2.9	2.10	2.11	2.12	2.13	2.14
SiO ₂	57.28	47.02	50.81	50.35	48.87	54.03	48.66
Al ₂ O ₃	15.74	12.83	14.13	12.22	14.69	14.76	12.41
Total Fe as Fe ₂ O ₃	8.02	11.26	11.00	10.83	11.25	9.85	11.28
MgO	6.42	16.07	9.68	14.49	11.51	7.26	16.02
CaO	5.27	9.17	8.86	8.63	8.18	7.15	7.91
Na ₂ O	2.11	1.19	2.50	1.24	2.11	3.23	1.31
K ₂ O	3.69	1.14	1.33	0.94	1.70	2.03	1.13
TiO ₂	0.83	0.84	1.11	0.75	1.00	1.07	0.75
MnO	0.08	0.19	0.17	0.21	0.20	0.15	0.22
P ₂ O ₅	0.26	0.23	0.33	0.25	0.31	0.28	0.25
S	0.30	0.08	0.10	0.09	0.17	0.19	0.06

Pb	36	ND	32	33	33	32	ND
Ba	3165	1481	1363	981	1041	1595	1221
Nb	7	4	3	4	7	7	3
Zr	87	48	73	44	57	67	44
Y	26	18	18	16	17	16	16
Sr	450	324	509	286	421	569	269
Rb	60	28	24	22	50	38	26
Zn	140	102	166	98	116	101	101
Cu	68	66	35	71	46	52	47
Ni	23	217	117	208	116	45	241
Cr	99	490	305	510	470	140	561
V	200	ND	200	175	220	207	ND

	2.15	2.16	2.17	2.18	2.19	2.20
SiO ₂	58.69	54.95	43.92	49.37	58.17	63.02
Al ₂ O ₃	11.05	15.80	13.10	14.91	14.93	13.95
Total Fe as Fe ₂ O ₃	7.52	9.41	12.80	9.99	6.49	7.36
MgO	5.66	5.79	15.71	11.76	3.07	3.30
CaO	12.45	6.36	9.07	6.68	9.04	4.88
Na ₂ O	1.47	3.71	2.24	3.62	5.93	4.83
K ₂ O	1.35	2.33	1.75	2.18	0.88	1.09
TiO ₂	0.85	1.01	0.87	0.90	0.82	0.82
MnO	0.20	0.15	0.22	0.15	0.16	0.10
P ₂ O ₅	0.44	0.30	0.29	0.32	0.34	0.29
S	0.33	0.21	0.02	0.12	0.17	0.35

Pb	33	33	ND	30	38	38
Ba	1875	1639	445	832	924	1098
Nb	5	5	3	5	9	7
Zr	80	77	46	50	109	84
Y	19	21	19	17	24	22
Sr	507	536	415	473	637	412
Rb	27	34	28	32	15	23
Zn	173	89	111	83	151	98
Cu	53	47	35	90	36	48
Ni	45	25	292	152	22	9
Cr	52	73	544	373	55	53
V	207	188	ND	175	175	156

B3	Sample No.	3.1	3.2	3.3	3.4	3.5	3.6	3.7
SiO ₂		72.45	72.36	76.59	75.79	73.75	70.97	68.59
Al ₂ O ₃		12.46	12.02	11.57	11.73	13.21	11.25	6.19
Total Fe as Fe ₂ O ₃		3.67	3.33	3.01	3.67	3.69	4.28	4.99
MgO		1.81	1.57	1.29	1.23	1.41	2.43	3.20
CaO		3.61	4.37	2.00	2.23	2.38	5.30	12.43
Na ₂ O		1.22	2.40	1.71	0.94	1.11	1.60	1.71
K ₂ O		3.66	2.97	2.98	3.48	3.87	3.14	1.66
TiO ₂		0.80	0.62	0.62	0.65	0.69	0.61	0.57
MnO		0.09	0.16	0.04	0.04	0.05	0.11	0.31
P ₂ O ₅		0.11	0.14	0.18	0.15	0.20	0.17	0.31
S		0.12	0.04	0.03	0.09	0.15	0.14	0.06
Pb		200	23	20	20	22	36	20
Ba		1421	1353	1275	1355	1371	969	589
Nb		18	14	13	14	15	12	11
Zr		260	177	206	182	205	154	182
Y		39	29	33	32	38	23	31
Sr		345	448	282	262	289	466	315
Rb		85	70	80	92	104	79	49
Zn		168	102	79	95	104	174	139
Cu		12	8	9	24	39	28	11
Ni		21	21	28	37	35	20	11
Cr		71	65	63	134	116	63	50
V		94	100	75	100	100	180	75

	3.8	3.9	3.10	3.11	3.12	3.13	3.14
SiO ₂	77.49	79.11	66.38	75.74	71.78	76.56	69.00
Al ₂ O ₃	10.74	5.93	11.53	12.76	5.20	12.46	16.40
Total Fe as Fe ₂ O ₃	3.43	2.72	5.77	3.69	3.50	2.70	3.18
MgO	1.11	1.66	2.25	0.96	3.20	0.70	1.49
CaO	1.97	6.59	7.38	1.38	12.70	1.55	2.48
Na ₂ O	1.98	2.28	3.10	1.68	1.57	2.40	2.34
K ₂ O	2.39	0.77	2.29	2.96	0.96	2.75	3.83
TiO ₂	0.56	0.35	0.61	0.53	0.42	0.48	0.69
MnO	0.05	0.26	0.24	0.04	0.44	0.02	0.02
P ₂ O ₅	0.16	0.30	0.38	0.13	0.20	0.09	0.18
S	0.11	0.02	0.06	0.14	0.04	0.29	0.40
Pb	22	23	43	35	40	25	25
Ba	829	199	818	1128	251	822	1095
Nb	13	8	10	12	10	11	15
Zr	181	252	149	150	317	121	222
Y	20	32	61	21	23	32	24
Sr	256	288	433	249	406	289	277
Rb	68	18	64	73	23	79	106
Zn	101	53	118	75	70	71	48
Cu	31	3	20	67	8	31	45
Ni	27	13	14	24	12	23	18
Cr	77	27	45	52	30	61	62
V	81	25	88	88	25	100	100

	3.15	3.17	3.19	3.20	3.21	3.23
SiO ₂	54.38	76.64	77.50	65.09	77.04	78.39
Al ₂ O ₃	12.15	12.71	4.22	3.69	11.62	9.20
Total Fe as Fe ₂ O ₃	9.84	4.05	2.21	2.85	3.48	3.14
MgO	7.86	0.93	2.07	5.38	0.86	1.31
CaO	9.19	0.58	10.82	19.57	0.75	3.32
Na ₂ O	2.69	1.82	1.51	1.09	3.54	1.64
K ₂ O	1.27	2.24	0.73	1.09	1.85	2.20
TiO ₂	1.59	0.61	0.22	0.27	0.57	0.51
MnO	0.15	0.02	0.08	0.38	0.02	0.05
P ₂ O ₅	0.49	0.36	0.50	0.50	0.12	0.18
S	0.39	0.03	0.14	0.08	0.16	0.06
Pb	ND	17	27	ND	23	20
Ba	763	617	159	154	740	927
Nb	20	17	8	8	7	12
Zr	129	145	214	141	138	130
Y	23	48	23	15	24	31
Sr	419	190	242	402	285	221
Rb	48	62	16	25	54	50
Zn	147	178	13	18	91	90
Cu	34	42	10	4	40	16
Ni	13	38	6	11	27	22
Cr	245	83	20	25	38	72
V	ND	175	25	ND	88	75

B4	Sample No.	4.1	4.4	4.5	4.6	4.7	4.8	4.9
SiO ₂		88.45	83.88	75.34	86.20	85.85	82.00	85.88
Al ₂ O ₃		5.88	9.27	14.17	7.23	7.49	10.35	7.07
Total Fe as Fe ₂ O ₃		1.45	1.06	3.25	1.63	1.35	1.94	1.94
MgO		0.34	0.32	1.01	0.39	0.25	0.46	0.53
CaO		0.95	1.28	0.22	0.74	1.14	0.55	1.22
Na ₂ O		1.81	2.94	1.15	2.43	2.67	2.01	2.20
K ₂ O		0.48	0.72	3.59	0.67	0.40	1.74	0.73
TiO ₂		0.28	0.32	0.59	0.38	0.37	0.40	0.36
MnO		0.01	0.01	0.02	0.02	0.01	0.02	0.02
P ₂ O ₅		0.14	0.05	0.16	0.13	0.13	0.17	0.14
S		0.20	0.16	0.49	0.18	0.34	0.37	0.20
Pb		21	33	27	20	27	23	23
Ba		46	114	727	59	38	361	80
Nb		10	11	16	11	11	11	9
Zr		252	124	196	254	272	182	239
Y		16	13	22	17	15	17	18
Sr		208	308	98	176	221	160	192
Rb		21	30	95	33	21	47	37
Zn		30	17	39	19	51	15	23
Cu		11	17	22	12	26	21	12
Ni		9	15	20	9	11	12	8
Cr		22	20	46	25	23	29	25
V		25	25	69	38	25	38	38

	4.10	4.11	4.12	4.13	4.14	4.15
SiO ₂	72.73	62.52	66.39	67.72	66.82	88.17
Al ₂ O ₃	15.17	21.93	18.34	17.11	17.22	5.74
Total Fe as Fe ₂ O ₃	4.28	3.99	5.31	5.06	5.13	2.74
MgO	0.99	1.43	1.56	1.55	1.73	0.48
CaO	0.70	1.67	1.01	1.50	1.97	0.47
Na ₂ O	1.16	1.85	1.53	2.05	2.50	1.41
K ₂ O	3.57	5.03	4.27	3.65	3.41	0.55
TiO ₂	0.76	1.20	0.93	0.91	0.93	0.23
MnO	0.02	0.06	0.06	0.06	0.07	0.02
P ₂ O ₅	0.14	0.12	0.13	0.13	0.14	0.08
S	0.48	0.21	0.48	0.26	0.08	0.11
Pb	33	47	37	40	43	23
Ba	947	1369	1073	840	683	74
Nb	19	28	25	21	22	7
Zr	277	254	276	299	290	141
Y	31	47	30	33	39	12
Sr	163	322	229	318	408	223
Rb	100	157	137	125	148	27
Zn	54	57	80	72	87	21
Cu	29	17	27	36	20	14
Ni	29	32	25	27	26	5
Cr	64	105	80	76	75	14
V	81	138	100	100	88	25

	4.16	4.17	4.18	4.19	4.20	4.21	4.22
SiO ₂	68.22	67.85	66.34	67.60	61.06	64.32	71.28
Al ₂ O ₃	17.62	18.08	17.50	17.99	19.06	18.98	14.67
Total Fe as Fe ₂ O ₃	5.78	5.94	7.61	5.87	6.36	6.45	6.92
MgO	1.48	1.43	2.15	1.42	2.50	1.83	1.77
CaO	0.35	0.21	0.34	0.51	3.25	1.27	0.61
Na ₂ O	0.98	0.94	0.67	1.03	2.76	1.42	1.01
K ₂ O	4.43	4.36	4.28	4.40	3.71	4.52	2.68
TiO ₂	0.90	0.91	0.83	0.91	1.00	0.93	0.75
MnO	0.06	0.05	0.07	0.05	0.07	0.06	0.07
P ₂ O ₅	0.13	0.14	0.13	0.12	0.13	0.13	0.13
S	0.07	0.10	0.10	0.12	0.09	0.10	0.12
Pb	35	33	30	37	47	38	33
Ba	826	765	753	746	848	837	555
Nb	25	20	23	25	21	25	19
Zr	279	262	202	279	179	222	313
Y	38	37	33	37	30	34	32
Sr	177	155	164	228	538	321	223
Rb	146	140	167	155	178	168	86
Zn	71	66	109	71	99	81	100
Cu	18	24	36	37	24	28	28
Ni	20	24	25	33	27	26	24
Cr	79	80	79	77	97	84	63
V	100	100	113	100	138	113	88

B5	Sample No.	5.1	5.2	5.3	5.4	5.5	5.6	5.7
SiO ₂		68.09	69.52	72.67	70.84	72.27	66.94	68.60
Al ₂ O ₃		14.09	13.71	8.16	12.19	10.94	11.33	4.65
Total Fe as Fe ₂ O ₃		5.65	2.88	3.42	3.99	4.30	5.20	2.59
MgO		3.23	3.04	2.95	3.01	2.69	3.51	4.64
CaO		1.63	3.38	7.75	3.34	4.22	6.74	15.06
Na ₂ O		1.27	2.16	2.18	2.78	2.59	1.90	1.16
K ₂ O		3.98	3.39	1.04	2.02	1.44	2.24	1.21
TiO ₂		0.52	0.67	0.55	0.65	0.38	0.54	0.37
MnO		0.06	0.07	0.09	0.05	0.05	0.06	0.10
P ₂ O ₅		0.25	0.31	0.53	0.18	0.39	0.69	1.26
S		1.24	0.87	0.65	0.94	0.72	0.86	0.35
Pb		40	37	27	33	30	43	ND
Ba		1123	1014	335	722	422	756	411
Nb		15	16	12	15	11	15	9
Zr		209	261	290	205	185	207	444
Y		31	36	39	37	31	50	47
Sr		138	207	162	259	218	199	308
Rb		109	82	26	89	48	47	19
Zn		155	24	220	71	98	144	36
Cu		46	55	41	71	39	61	34
Ni		78	68	81	31	31	82	11
Cr		98	114	73	79	46	76	41
V		150	175	100	150	113	250	ND

	5.8	5.9	5.11	5.12	5.13	5.14	5.15
SiO ₂	66.52	60.13	59.64	65.20	68.40	63.99	65.06
Al ₂ O ₃	13.78	4.57	14.46	14.62	12.99	14.95	11.46
Total Fe as Fe ₂ O ₃	4.34	3.24	4.87	4.11	4.18	5.56	5.64
MgO	2.62	5.35	5.94	4.81	4.06	3.72	3.78
CaO	5.57	22.63	7.22	4.60	4.10	4.97	8.22
Na ₂ O	1.17	0.89	2.48	1.68	1.89	2.77	1.97
K ₂ O	4.25	1.71	2.67	3.50	2.84	2.52	2.41
TiO ₂	0.70	0.48	0.90	0.76	0.67	0.61	0.54
MnO	0.04	0.17	0.07	0.07	0.05	0.05	0.08
P ₂ O ₅	0.33	0.45	1.01	0.16	0.27	0.25	0.32
S	0.68	0.38	0.74	0.50	0.55	0.62	0.52
Pb	33	ND	35	30	60	37	37
Ba	1283	537	1259	1435	1033	1085	950
Nb	15	10	21	17	19	11	11
Zr	166	264	273	252	232	136	112
Y	50	28	83	28	36	23	35
Sr	224	255	354	244	253	408	279
Rb	113	32	79	105	100	84	
Zn	737	452	284	160	108	159	
Cu	79	30	73	61	60	69	60
Ni	94	31	81	37	49	19	35
Cr	190	71	170	123	156	79	142
V	882	ND	250	163	219	231	350

b) Mineral assemblages in samples from the sedimentary groups (in approximate order of abundance)

B1	B2	B3
plagioclase	plagioclase	quartz
quartz	actinolite	plagioclase
chlorite	quartz	biotite
opaque oxides	biotite	opaque oxides
calcite	opaque oxides	calcite
	calcite	
B4	B5	
quartz	quartz	
biotite	plagioclase	
chlorite	anthophyllite	
opaque oxides	cordierite	
calcite		

	5.16	5.17	5.18	5.19	5.20	5.21
SiO ₂	60.20	62.12	65.08	63.03	50.80	28.90
Al ₂ O ₃	15.86	19.14	13.86	15.26	9.54	0.50
Total Fe as Fe ₂ O ₃	7.13	6.11	5.62	6.19	6.38	5.45
MgO	3.97	2.77	3.38	3.69	4.16	14.92
CaO	5.56	1.46	5.45	4.44	22.89	48.51
Na ₂ O	3.85	1.55	2.10	2.82	2.70	0.12
K ₂ O	1.71	5.14	2.96	2.84	1.70	0.37
TiO ₂	0.58	0.74	0.67	0.66	0.70	0.19
MnO	0.05	0.03	0.05	0.05	0.24	0.57
P ₂ O ₅	0.20	0.20	0.26	0.21	0.28	0.40
S	0.87	0.74	0.57	0.81	0.60	0.06
Pb	40	30	32	35	ND	ND
Ba	337	2983	1545	1059	909	1001
Nb	7	11	14	12	8	5
Zr	97	116	152	112	128	74
Y	26	31	36	33	25	12
Sr	445	112	295	423	487	625
Rb	67	109	83	95	44	4
Zn	195	534	323	510	103	70
Cu	95	83	66	83	51	13
Ni	32	39	36	34	13	7
Cr	79	167	136	125	35	26
V	213	525	313	325	ND	ND

c) Norms for the average chemical composition of the sedimentary groups

	B1	B2	B3	B4	B5
Qt	13.6	0.9	42.9	36.8	26.1
Or	13.7	10.2	14.9	15.7	16.7
Ab	28.2	30.8	16.2	13.1	18.8
An	19.8	18.9	12.6	20.1	19.1
Di	4.3	12.4	6.6	--	4.4
Hyp	16.1	21.9	4.3	5.8	11.7
Mt	2.8	3.4	1.3	1.6	1.9
Ilm	1.5	1.7	1.2	1.2	1.2
Cor	--	--	--	5.7	--

B30233